Biofacies, taphofacies, and depositional environments in the north of Neotethys Seaway (Qom Formation, Miocene, Central Iran)

Mahdiyeh Mahyad, Amrollah Safari *, Hossein Vaziri-Moghaddam, Ali Seyrafian

Department of Geology, Faculty of Sciences, University of Isfahan, Isfahan, 81746-73441, Iran

*Corresponding author
E-mails address: safari@sci.ui.ac.ir; a.safari901@gmail.com

Abstract:

This research attempted to reconstruct the sedimentary environment and depositional sequences of the Qom Formation in Central Iran, using biofacies and taphofacies analyses. The Qom Formation in the Andabad area with 220 m of thickness is located at N 3°48'12.6" and E 47°59'28". The thickness of the Qom Formation in the Nowbaran area (N 35°05'22.5" and E 49°41'00") was found to be 458 m. In both areas, the formation mainly consists of shale and limestone. The lower boundary between the Qom and Lower Red formations is unconformable in both areas. In the Nowbaran area, the Qom Formation is covered by recent alluvial sediments. In the Andabad area, the Qom Formation was unconformably overlaid by the Upper Red Formation. A total of 122 limestone and 15 shale rock samples were collected from the Andabad area, and 94 limestone and 24 shale rock samples were collected from the Nowbaran area. Analysis of the collected samples resulted in the recognition of nine biofacies, one terrigenous facies, and five taphofacies within the Qom Formation in the both areas. Based on the vertical distributions of biofacies, the Qom Formation is deposited on an open shelf carbonate platform. This carbonate platform can be divided into three subenvironments: inner shelf (restricted and semi-restricted lagoon), middle shelf, and outer shelf. Two third-order and one incomplete depositional sequences were identified in the Nowbaran area, but in the Andabad area, three third-order and one incomplete depositional sequences were distinguished.

Keywords: Biofacies; taphofacies; Nowbaran area; Andabad area; Qom Formation; Neotethys Seaway.

1 Introduction

Central Iran zone is one of the eight structural-sedimentary zones introduced by Berberian and King (1981) and Heydari (2008) (Fig. 1a). The researchers divided the Iranian plateau into eight structural-sedimentary zones: Zagros, Sanandaj-Sirjan, Urumieh-Dokhtar magmatic arc, Alborz, Central Iran, Lut, Kopeh Dagh, and Makran (Berberian and King, 1981; Heydari, 2008). Central Iran zone is located in the Alpine-Himalayan orogenic belt and is bounded from north and south by Paleotethys and Neotethys Ocean suture zones (Aghanabati, 2006; Nadimi, 2007). The Oligocene–Miocene deposits (Qom Formation) were reported in different areas of the Central Iran zone (Schuster and Wielandt, 1999; Harzhauser, 2004; Khaksar and Maghfouri Moghadam, 2007; Daneshian and Dana, 2007; Reuter et al., 2009; Behforouzi and Safari, 2011; Moghadam, 2011; Mohammadi et al., 2011; Seddighi et al., 2011; Yazdi et al., 2012; Mohammadi et al., 2013; Abbassi et al., 2016; Rahiminejad et al., 2017; Daneshian and Ghanbari, 2017; Mohammadi et al., 2018). However, studies on the Qom Formation were focused on biostratigraphy and paleontology (Khaksar and Maghfouri Moghadam, 2007; Daneshian and Dana, 2007; Behforouzi and Safari, 2011; Moghadam, 2011; Abbassi et al., 2016; Daneshian and Ghanbari, 2017), paleoecology (Schuster and Wielandt, 1999; Harzhauser, 2004; Yazdi et al., 2012; Rahiminejad et al., 2017), and biofacies and sedimentary environment (Mohammadi et al., 2011; Seddighi et al., 2011; Mohammadi et al., 2013; Mohammadi et al., 2018). On the other hand, studies of sequence stratigraphy and taphofacies analysis were not conducted in the Qom Formation. In 1972 and 1976, the concept of biofacies was developed (Flugel, 1972; Wilson, 1976). Subsequently, the biofacies analysis was used for the reconstruction and interpretation of sedimentary environments (Flugel, 1982; Flugel, 2010). However, the influence of taphonomic processes (e.g. grain dispersal and distribution) was not considered in reconstruction of sedimentary environments based on biofacies analysis (Brachert et al., 1998). Therefore, Brachert et al. (1998) introduced the term ‘taphofacies’ term. In 2011, the concept of taphofacies was developed and applied to reconstruction and interpretation of paleoenvironmental conditions based on taphonomic processes (Silvestri et al., 2011). Therefore, the objectives of the present

study include 1) identification of biofacies and taphofacies in the Miocene sediments of Qom basin, and 2) reconstruction of sedimentary environment and identification of depositional sequences in the Qom Formation and correlation between these depositional sequences and the sequences formed at the southern margin of the Neotethys basin and of the Paratethys Basin.

2 Geological setting

During the Eocene and Early Oligocene, an uplift and volcanic activity resulted in a continental environment in the studied area (Morley et al., 2009). Subsidence caused by cooling of the upper mantle led to a marine flooding during the Early Oligocene in the Central Iran zone (Morley et al., 2009). Reuter et al. (2009) and Harzhauser and Piller (2007) pointed out that the Qom Sea was shallow, connecting the eastern and western basins of Neotethys. Urumieh-Dokhtar magmatic arc created two sub-basins (a fore-arc Esfehan-Sirjan Basin) and a back-arc Qom Basin) in the Central Iran zone during the Oligocene and Miocene (Reuter et al., 2009) (Fig. 1b). The Qom Formation in the studied areas represented the back-arc sub-basin (Qom Basin) (Fig. 1c). The Qom Formation is distributed over a large area of the Central Iran zone (Aghanabati, 2006). Unfortunately, due to the different sedimentary facies in the Central Iran zone, the type-section for this formation has not been designated. In the Qom area, this formation is 1200-m-thick and consists primarily of evaporite, siliciclastic, and carbonate sediments. Loftus (1854) was the first to study this formation. In the Qom area, Furrer and Soder (1955), and Gansser (1955) divided the Qom Formation into 6 members (A, B, C, D, E, and F). Abaie et al. (1964) identified 4 members: C1, C2, C3, and C4. The Qom Formation in the Andabad area unconformably overlies the Lower Red Formation. The upper boundary of the Qom Formation with the Upper Red Formation in the area under study is unconformable. Deposits of the Qom Formation in the Andabad area contain shale (lower section) and limestone (upper section). In the Nowbaran area, the deposits of the Qom Formation include the alternation of shale and limestone in the lower section, and layers of limestone in the middle section. In the upper section of the sequence under study, alternation of shale and limestone can be observed. The lower boundary of the Qom Formation with the Lower Red Formation is unconformable in the Nowbaran area. The upper boundary of the Qom Formation in the study area is concealed under recent alluvial deposits.

Text-Fig. 1

3 Materials and Methods

The Nowbaran area (N 35°05’22.5”; E 49°41’00”) is located 3 km from Nowbaran (northeast of Saveh) (Fig. 2), whereas the Andabad area (N 36°48’12.6”; E 47°59’28”) is located 19 km northeast of Mahneshan (Fig. 2). A total of 122 (limestone) and 15 (shale) rock samples were collected from the Andabad area, and 94 (limestone) and 24 (shale) rock samples were collected from the Nowbaran area in order to determine biofacies, taphofacies, sedimentary environment, and depositional sequences of the Qom Formation. Thin sections were produced from the rock samples. Microfossils were extracted from shales using 10% water solution of hydrogen peroxide (H_2O_2), and then picked from soaked and dried residue. The biofacies of both areas were identified based on sediment texture, grain size, grain composition, and fossil content. Sedimentary textures in thin sections were identified using the classification system of Dunham (1962) and Embry and Klovan (1971). The abundance of larger benthic foraminifera, coral, bryozoan, and coraline red algae in the Andabad and Nowbaran areas can be used to study biofacies and identify taphofacies. Therefore, taphonomic signatures such as fragmentation, abrasion, encrustation, and bioerosion have been determined by several researchers (Allison and Bottjer, 2011; Silvestri et al., 2011). In studies by Silvestri et al. (2011) and Bover-Arnal et al. (2017), the qualitative estimation of taphonomic signatures (pre-burial stage) was performed in the thin sections. The classification was introduced to assess qualitatively, of the damaged test of large benthic foraminifera, by waves and water energy (Beavington-Penny, 2004). This qualitative classification includes four categories: (0) pristine and undamaged test margin of large benthic foraminifera; (1) damaged outer margin in large benthic foraminifera test on both sides and outer margin irregularly in large benthic foraminifera test; (2) destroyed outer wall in large benthic foraminifera test and damaged test on both sides; and (3) very damaged test belonging to symbiont-bearing larger benthic foraminifera and test fragmented into small pieces. The qualitative evaluation of damaged test of large benthic foraminifera in the areas under study was performed using the classification method introduced by Beavington-Penny (2004). To identify taphofacies in the areas under study, several resources are used (e.g. Brachert et al.,

1998; Allison and Bottjer, 2011; Silvsteri et al., 2011; Nebelsick and Bassi, 2000; and Nebelsick et al., 2011). The researchers pointed out that thickness to diameter ratio of the test of the genus *Amphistegina* varies with increasing seawater depth (Larsen and Drooger, 1977; Hallock and Hansen, 1979; Hallock and Glenn, 1986; Hallock, 1999; Mateu-Vicens et al., 2009). Mateu-Vicens et al. (2009) showed that the ratio of thickness to diameter of the test in the genus *Amphistegina* can be used as an indicator for seawater depth. By measuring the thickness/diameter ratio of the test in the *Amphistegina* genus (in axial and subaxial section) in microscopic thin sections and calculating the morphological changes of the test using this formula "Zom = 2.046 T/D-2.293", under oligo-mesotrophic condition, a diagram can be drawn to predict *Amphistegina* genus test changes with seawater depth (Mateu-Vicens et al., 2009). The diagram depicted the oligo-mesotrophic condition and can be used to determine the seawater depth of the past geological age (especially for Oligocene–Miocene). In the area under study, eighty-five representatives of the genus *Amphistegina* were chosen. The diameter and thickness of tests were measured in axial and subaxial sections. Of these samples, 26 belonged to the Andabad area while 59 belonged to the Nowbaran area. Then, the thickness to diameter ratio was calculated for each sample. In the areas under study, the depth of seawater was calculated for the *Amphistegina* genus-bearing biofacies using the method of Mateu-Vicens et al. (2009). The curves of the depth of seawater were drawn for both areas under study (Figs. 6 and 7).

Text-Fig. 2

4 Results

4.1 Description of Biofacies

Based on type and distribution of components, sedimentology and petrography characteristics nine biofacies and one terrigenous facies belonging to the Andabad and Nowbaran areas were identified. MF-1: Sandy bioclast wackestone-packstone (MF-1) was observed in both areas under study (Fig. 3a). The main components of this biofacies are skeletal (miliolids, bivalve, ostracod, and echinoderm) and clastic (fine-grained quartz). Imperforate foraminifera such as *Borelis*, *Archaias*, *Peneroplis*, and *Meandropsina* are the subordinate components of MF1 biofacies. MF-

2: The abundance of imperforate foraminifera (miliolids, *Borelis*, *Archaias*, and *Sorites*) and red algae Corallinaceae in the Andabad area marks the bioclast Corallinaceae imperforate foraminifera wackestone-packstone (MF2) (Fig. 3b). The minor components of this biofacies are corals, bryozoans, gastropods, echinoderms, bivalves, and ostracods. MF-3: Bioclast Corallinaceae perforate-imperforate foraminifera wackestone-packstone (MF3) was observed in the Andabad and Nowbaran areas (Fig. 3c). The main components of this biofacies are imperforate foraminifera (miliolids, *Borelis*, *Archaias*, *Penarchaias*, *Peneroplis*, *Dendritina*, and *Meandropsina*), perforate foraminifera (*Amphistegina*, *Neorotalia*, *Heterostegina*, and *Miogypsina*), and red algae Corallinaceae. The debris of corals, bryozoans, gastropods, echinoderms, bivalves, ostracods, and small Rotalia are the subordinate components of the Bioclast Corallinaceae perforate-imperforate foraminifera wackestone-packstone biofacies (MF3). The thickness to diameter ratio of test in the *Amphistegina* genus in the MF 3 biofacies is 0.44 mm in the Nowbaran area and reaches 0.45 mm in the Andabad area (Tables 1 and 2). MF-4: Coral is the only allochem that forms coral boundstone (MF 4) (Fig. 3d). The corals in this biofacies were observed as patch reefs and these patch reefs are discontinuous as well as scattered colonies in both areas. Areas between the coral colonies are filled with sediment containing bivalve, corallinaceae algae, and gastropods, as well as foraminifera such as miliolids and *Amphistegina*. In the Nowbaran area, the thickness to diameter ratio of test in the *Amphistegina* genus is 0.4 mm for the biofacies MF4 (Table 2). MF-5: Coral and corallinaceae algae are the abundant components that exist in the coral corallinaceae wackestone-packstone (MF5) (Fig. 3e). Perforate foraminifera (*Miogypsina*, *Amphistegina*, and Rotalidae family), imperforate foraminifera (miliolids, *Borelis*, and *Dendritina*), gastropods, echinoderms, bivalves, and ostracods are minor components in the biofacies (MF 5). Thus, the biofacies were observed in both areas under study and the thickness to diameter ratios of test in *Amphistegina* genus in the Andabad and Nowbaran areas were 0.4 and 0.34 mm, respectively (Tables 1 and 2). MF-6: In both areas, bioclast corallinaceae perforate foraminifera wackestone-packstone (MF6) consisted of several main components such as red algae corallinaceae, bryozoan, and perforate foraminifera (*Amphistegina*, *Neorotalia*, *Heterostegina*, *Miogypsina*, and *Lepidocyclina*) (Fig. 3f). The subordinate components of this biofacies were corals, bivalves, miliolids, and echinoderms. Bryozoans were found to be abundant in some samples obtained from the Nowbaran area. The thickness to diameter ratio of test in the measured samples of *Amphistegina*

genus was 0.23 mm in the Nowbaran area, and this ratio reached 0.36 mm in the MF6 biofacies of the Andabad area (Tables 1 and 2). MF-7: Corallinaceae, bryozoan, perforate foraminifera (*Amphistegina*, *Neorotalia*, *Heterostegina*, *Miogypsina*, and *Lepidocyclina*), and planktonic foraminifera are the main components of the bioclast corallinaceae pelagic-perforate foraminifera wackestone-packstone (MF7) (Fig. 3g). Symbiont-bearing larger benthic foraminifera are abundant in this biofacies. Corals, bivalves, ostracods, and echinoderms are the minor components of this biofacies. MF7 was only found in the Nowbaran area, and the thickness to diameter ratio of the test in the *Amphistegina* genus of this biofacies reached 0.33 mm (Table 2). MF-8: Bioclast pelagic benthic foraminifera wackestone-packstone (MF8) mainly consisted of perforate foraminifera (*Amphistegina*, *Heterostegina*, *Operculina*, and *Neorotalia*) and planktonic foraminifera (Fig. 3h). Corallinaceae algae, bivalves, and echinoderms can be subordinate components in this biofacies. MF8 was only found in the Nowbaran area. The thickness to diameter ratio of test in the *Amphistegina* genus of MF8 reached 0.31 mm (Table 2). MF-9: Planktonic foraminifera are the main components of the bioclast pelagic foraminifera wackestone-packstone (MF9) (Fig. 3i). The minor components of this biofacies contained *Neorotalia*, bivalves, and echinoderms. MF9 was only found in the Andabad area.

Text-Fig. 3

Table 1

Table 2

4.2 Terrigenous Facies (Shale)

The thickly laminated grey shale can be observed in the study areas. In the Nowbaran area, this terrigenous facies alternates with the lagoon biofacies (MF1 and MF4). Also, this facies alternates with the lagoon biofacies (MF2 and MF4) in the Andabad area. This terrigenous facies contained perforate foraminifera (*Elphidium*, *Amphistegina*, *Discorbis*, and small *Rotalia*), imperforate foraminifera (miliolids and *Borelis*), bryozoans, and ostracods.

4.3 Taphofacies Analysis

Five taphofacies were identified in the Andabad and Nowbaran areas. These taphofacies are categorized based on their main components and taphonomic signatures including fragmentation, bioerosion, encrustation, disarticulation, and abrasion. MTF-1: taphofacies 1 contains Corallinaceae and imperforate large benthic foraminifera (*Borelis*, *Peneroplis*, *Archaias*, and *Sorites*). This taphofacies was only found in the Andabad area. The taphofacies 1 showed moderate to high fragmentation and disarticulation rates (Figs. 4a). Bioerosion and encrustation rates were low and low to moderate, respectively. Also, the taphofacies 1 showed various abrasion rates from low to high. In the Andabad area, the rate of damage incurred to walls of large benthic foraminifera in the taphofacies 1 was high (category 2 to 3). Moreover, red algae Corallinaceae, corals, perforate foraminifera (*Amphistegina*, *Neorotalia*, *Heterostegina*, and *Miogypsina*), and imperforate foraminifera (*Borelis*, *Peneroplis*, *Archaias*, and *Penarchaias*) are the abundant components in the taphofacies 2. MTF-2: taphofacies 2 was found in both Andabad and Nowbaran areas (Figs. 4b and 5a). The Nowbaran area showed moderate rates of fragmentation and disarticulation, as well as abrasion, but there was no bioerosion. The encrustation rate in the taphofacies 2 in the Nowbaran area was low to moderate, while the abrasion and encrustation rates in the taphofacies 2 in the Andabad area were low to moderate. The Andabad area showed low rate of Bioerosion. The fragmentation and disarticulation rate of Corallinaceae and corals in the taphofacies 2 varied from low to high. In the Nowbaran area, the rate of damage incurred to the outer shell of large benthic foraminifera varied from low to moderate (category 1 to 2), while in the Andabad area, it was high (category 2 to 3). MTF-3: taphofacies 3 was found both in the Nowbaran and Andabad areas, and this taphofacies mainly consisted of corals (Figs. 4c and 5b). The rates of taphonomic signatures including fragmentation, abrasion, and encrustation, were lower in both areas. The taphofacies 3 showed a low rate of bioerosion only in the Nowbaran area. MTF-4: taphofacies 4, which was found in both areas, showed abundant Corallinaceae and corals. In both study areas, the taphofacies 4 showed low to moderate fragmentation and abrasion rates. The taphofacies 4 contained moderate to high rate of encrustation. This taphonomic feature was found in both study areas (Figs. 4 d and 5c); in the Nowbaran area, similar to Corallinaceae, bryozoans encrusted various types of allochems. In both areas, multilayered encrustation was found around various types of skeletal

grains. The taphofacies 4 showed a low rate of bioerosion in the Andabad area, and a low to moderate in the Nowbaran area. MTF-5: The abundance of Corallinaceae, corals, bryozoans, and large perforate foraminifera (*Amphistegina*, *Neorotalia*, *Heterostegina*, *Operculina*, and *Miogypsina*) marked the taphofacies 5 in both study areas (Figs. 4e and 5d). The fragmentation rates in both areas were moderate to high. The Nowbaran area showed low to moderate rates of abrasion and encrustation. However, the Andabad area showed moderate and low rates of abrasion and encrustation, respectively. Both areas showed low rates of bioerosion.

Text-Fig. 4

Text-Fig. 5

5 Depositional environments and sequences

5.1 Reconstruction of carbonate platform based on biofacies and taphofacies

Based on the distribution of benthic and pelagic foraminifera, vertical changes in biofacies, as well as the absence of bioclast, ooid, and reef barrier, an open-shelf carbonate platform can be considered for the Qom Formation in the studied areas (Figs. 6, 7, and 8). A carbonate ramp (particularly, a homoclinal carbonate ramp) interpretation has been excluded from the consideration because of the absence of diagnostic bioclast, ooid, and reef barrier deposits (Read, 1982; Read, 1985; Flugel, 2010). The open-shelf platform can be divided into three environments: inner shelf, middle shelf, and outer shelf. The inner shelf also includes sub-environments such as a restricted and a semi-restricted lagoon. Wilson and Evans (2002) pointed out that a biofacies similar to the sandy bioclast wackestone-packstone (MF1) could be formed in nearshore lagoonal settings. Also, carbonate deposits containing siliciclastic grains could be formed in swamps found within shallow coastal waters of a lagoon environment (Flugel, 2010; Pomar et al., 2015). The presence of skeletal (miliolids and gastropod) and clastic allochems (quartz) indicated that this biofacies (MF 1) was deposited in a restricted lagoon with high salinity seawater (Romero et al., 2002; Wilson and Evans, 2002). Imperforate foraminifera and red algae Corallinaceae indicated the existence of a high-energy shallow semi-restricted lagoon

with seagrass meadows for the bioclast Corallinaceae imperforate foraminifera wackestone-packstone (MF2) (Beavington-Penney et al., 2004; Renema, 2006; Tomassetti et al., 2016; Pomar et al., 2017). Biofacies similar to MF2 were identified in the Asmari and Jahrum formations (Vaziri Moghaddam et al., 2006; Taheri, 2010; Taheri et al., 2008). The presence of imperforate-perforate foraminifera and red algae corallinaceae, a semi-restricted lagoon with seagrass meadows can be demonstrated for the bioclast corallinaceae perforate-imperforate foraminifera wackestone-packstone (MF3) (Romero et al., 2002; Beavington-Penney et al., 2006; Afzal et al., 2011; Nebelsick et al., 2013). In the Nowbaran and Andabad areas, MF3 sediments were deposited in a shallow lagoon with ~8.5 and ~13 m depth. Terrigenous facies of the studied areas consisted of perforate foraminifera (*Elphidium*, *Amphistegina*, *Discorbis*, and small *Rotalia*) and imperforate foraminifera (miliolids and *Borelis*) which are indicative of the semi-restricted lagoon environment for this terrigenous facies (Geel 2000). In the studied areas, coral colonies (MF4) were observed as small patch reefs. Riegl et al. (2010) argued that such small patch reefs are formed in an environment with high level of water salinity and influx of siliciclastics. In addition, patch reefs characterise lagoon environment (Beresi et al., 2016). Other researchers found biofacies similar to MF4 in the Qom and Asmari formations (Mohammdi et al., 2011; Seddighi et al., 2011; Amirshahkarami et al., 2007). In the Nowbaran area, given the T/D ratio of the genus *Amphistegina*, MF4 was found in an environment with an estimated depth of ~19 m. Biofacies, such as MFs 2, 3, and 4, were formed in the inner shelf and above the fair weather wave base. Similarities in major allochems suggested that MTFs 1, 2, and 3, too, were formed in a shallow lagoon environment. Nebelsick et al. (2011) believed that fragmentation is in direct relationship with wave base and seawater depth so that the highest fragmentation rate could be observed in the inner shelf (lagoon). In the present study, the moderate rate of fragmentation indicates low to high energy levels of sedimentation environment (Nebelsick et al., 2011). Moderate to high fragmentation and abrasion rates in taphofacies 1 indicate high energy level of sedimentation environment, while low to moderate encrustation and bioerosion rates of this taphofacies in the Andabad area indicate lack of proper sedimentation condition for growing corallinaceae algae and burrowing microorganisms. Severe fragmentation of large benthic foraminifera and destruction of the outer wall and marginal cord of these foraminifera (category 2 and 3) are indicative of either high transportation of their test by sea wave or their test destruction by fishes and other destructive organisms (Beavington-Penny, 2004). Low-

moderate to high fragmentation and abrasion rates of taphofacies 2 in the Andabad area represent a low to high energy environment. Given the fragmentation and abrasion rates of the Nowbaran area, an environment with higher energy can be expected compared to the Andabad area. This is indicative of the higher water depth in the Andabad area. The low to moderate fragmentation rate (categories 1 and 2) of test (large benthic foraminifera) in the Nowbaran area, as compared to the moderate to high fragmentation rate (category 2 and 3) of test (large benthic foraminifera) in the Andabad area showed that the test in these animals in the latter area were more intensely reworked by waves compared to the Nowbaran area. Low taphonomic signature rates of fragmentation, bioerosion, encrustation, disarticulation, and abrasion, in both study areas, showed that taphofacies 3 were formed below wave base. This is consistent with the depth estimated for the patch reefs (MF4) (~19 m). The coral coralinaceae wackestone-packstone (MF5) and bioclast corallinaceae perforate foraminifera wackestone-packstone (MF6) were deposited in the proximal middle shelf environment. The abundance of coral and corallinaceae in MF5, a middle shelf with mesophotic-oligophotic condition can be expected for this biofacies (Pomar et al. 2017). The biofacies MF5 was formed under a high energy condition (near and below fair weather wave base) and in the middle shelf environment (Pomar, 2001; Flugel, 2010; Sarkar, 2017). The biofacies MF 5 were formed at water depth of ~29 m in the Nowbaran area and ~19 m in the Andabad area. This suggests that the seawater in the Nowbaran area was deeper than the Andabad area. The bioclast corallinaceae perforate foraminifera wackestone-packstone (MF6) contained red algae corallinaceae, bryozoan, and perforate foraminifera (*Amphistegina*, *Neorotalia*, *Heterostegina*, *Lepidocyclina*, and *Miogypsina*) and was deposited in a proximal middle shelf environment with the oligo-mesotrophic conditions (Brandano et al., 2012; Brandano et al., 2016; Sarkar, 2017). The T/D ratio of the genus *Amphistegina* in the biofacies MF6 suggests seawater depth of ~30 m in the Nowbaran area and ~25 m in the Andabad area. The bioclast corallinaceae pelagic-perforate foraminifera wackestone-packstone (MF7) and the bioclast pelagic benthic foraminifera wackestone-packstone (MF8) were formed in distal middle shelf environment in the Nowbaran area. Basically, the presence of large perforate foraminifera such as *Heterostegina*, *Operculina*, *Neorotalia*, *Miogypsina*, and *Amphistegina* indicate a middle shelf environment with the oligophotic condition (Brandano et al., 2012; Pomar et al., 2014). Biofacies such as MF7 and MF8 contained large perforate foraminifera (*Heterostegina*, *Operculina*, *Neorotalia*, *Miogypsina*, and *Amphistegina*), corallinaceae, and planktonic

foraminifera. Yet, this biofacies belongs to a distal middle shelf environment with the oligophotic condition (Brandano et al., 2012; Sarkar, 2017). The T/D ratio of *Amphistegina* genus in MF7 and MF8 suggests deposition at depth of ~30 and ~34.5 m in the Nowbaran area. The bioclast pelagic foraminifera wackestone-packstone (MF9) was deposited on the outer shelf environment in the Andabad area (Geel, 2000; Knoerich and Mutti, 2003). The presence of abundant planktonic foraminifera in MF9 is indicative of a deep basin (outer shelf). The main allochems of MTFs 4 and 5 are very similar to MFs 5, 6, 7, and 8. Yet, the taphofacies 4 was formed in the proximal middle shelf environment, and the taphofacies 5 was formed in the proximal to distal middle shelf environment. As a result of great similarity with MF5, the taphofacies 4 was formed at water depths of ~29 and ~19 m in the Nowbaran and Andabad areas. At a depth of 20 m, encrustation reached its highest rate (Greenstein and Pandolfi, 2003). Moreover, a high rate of encrustation is indicative of high energy environment and low sedimentation rate (Silvestri et al., 2011; Ćosović et al., 2012; Bover-Arnal et al., 2017). The encrustation rates in both areas were moderate to high suggesting a high energy environment with low sedimentation rate. In the Nowbaran area, similar to corallinaceae, bryozoans encrusted corals and other skeletal grains. Such encrustation is only seen in a moderate to high energy setting (Berning et al., 2009). Meanwhile, multi-layer encrustation was observed in both areas where corallinaceae were replaced with bryozoans during the encrusting process. This indicates a change in the environmental condition. Moderate to high rates of fragmentation and abrasion in the taphofacies 5 may be indicative of a high energy setting, while moderate fragmentation rate suggests a middle shelf setting. By analogy with MF6, the taphofacies 5 was deposited at water depth of ~25 m. Also similar to MFs 6, 7, and 8, this taphofacies was formed at ~30–34.5 m water depth in the Nowbaran area. Fragmentation of the tests of large perforate foraminifera was moderate (category 2) in the Andabad area, but in the Nowbaran area, it varied from low to high (category 1 to 3). As a result, the dispersal rate of large perforate foraminifera tests in the Andabad area was higher compared to Nowbaran area.

Text-Fig. 6

Text-Fig. 7

Text-Fig. 8

5.2 Sequence Stratigraphy

The end of the 20th century witnessed the definitions of components and conceptual models of sequence stratigraphy (Van Wagoner et al., 1988; Sarg, 1988; Handford and Loucks, 1993). Within this conceptual framework, Catuneanu et al. (2011) defined lowstand systems tract (LST), transgressive systems tract (TST), highstand systems tract (HST), and falling-stage systems tract (FSST). In the Nowbaran area, two third-order depositional sequences and one incomplete depositional sequence have been recognised in the Aquitanian Stage. On the other hand, three third-order depositional sequences and one incomplete depositional sequence (Burdigalian Age) have been identified in the Andabad area (Figs. 6 and 7).

Sequence 1

This sequence (Aquitanian Age) was identified in the Nowbaran area (Figs. 9 and 7). It reaches the thickness of 96 m and consists of alternating shale and limestone. The sequence boundary between this sequence and the Lower Red Formation is the Type I sequence boundary. This sequence boundary is an unconformity boundary. Additionally, the erosional surface of this sequence boundary can be observed between sandstone of the Lower Red Formation and shales of the Qom Formation. Sequence 1 began with terrigenous facies (shale) indicative of a lagoonal setting. The transgressive systems tract (TST) of this sequence consisted of alternating shale and limestone deposited in the lagoon environment. In terms of biofacies, the TST included lagoonal biofacies (sandy bioclastic wackestone-packstone biofacies MF1) and a terrigenous facies (shale). The bioclast pelagic benthic foraminifera wackestone-packstone biofacies (MF8) indicated the maximum flooding surface (MFS) of the sequence 1. The maximum water depth in the sequence 1 reached ~34.5 m. Biofacies such as MFs 4, 5, 6, 7, and 8 were deposited as a highstand systems tract (HST). The HST contains limestones deposited in inner and middle shelf settings. The sequence boundary between the first and second sequences was marked by the coral boundstone (MF4). This sequence boundary is a sequence boundary of Type II, because no erosional surface has been seen between the first and second sequences.

Text-Fig. 9

Sequence 2

Sequence 2 reaches 109 m in thickness and consists primarily of limestone deposited in the Nowbaran area during the Aquitanian Age (Figs. 7 and 10). It starts with the bioclast corallinaceae perforate foraminifera wackestone-packstone (MF6). The transgressive systems tract (TST) consisted of open marine biofacies (MFs 5, 6, and 7) represented by limestones (middle part of the studied succession) deposited in a middle shelf environment. The bioclast corallinaceae pelagic-perforate foraminifera wackestone-packstone (MF7) marks the maximum flooding surface (MFS) for the sequence 2. The estimated water depth reached ~30 m in this sequence. The highstand systems tract (HST) in this sequence included MFs 1, 3, 4, 5, 6, and 7. This systems tract (HST) contains limestones of the lagoon and middle shelf environment characterised by the absence of terrigenous sediment input. Sequence boundary between the second and third sequences was marked by the sandy bioclast wackestone-packstone (MF1). This sequence boundary is marked by limestone of the lagoon environment. The sequence boundary between the second and third sequences is Type II sequence boundary.
Text-Fig. 10

Sequence 3

This is an incomplete aggradation sequence reaching 255 m thickness formed in the Nowbaran area (Figs. 7 and 11). Sequence 3 was formed during the Aquitanian Age and mainly consisted of lagoon shale and limestone. The maximum water depth did not exceed ~8.5 m, and this sequence included the sandy bioclast wackestone-packstone (MF1), as well as the terrigenous facies (shale). The upper boundary of this sequence in the Nowbaran area was Type I sequence boundary which separates the Qom Formation from the Recent Alluvial Sediments. The erosional surface between this sequence (Qom Formation) and the Recent Alluvial Sediments can be observed. This erosional surface indicates that the Qom Formation was not deposited during the Burdigalian Age.
Text-Fig. 11

Sequence 4

Type I sequence boundary separates the first sequence of the Qom Formation from the Lower Red Formation and is characterized by an erosional surface. Sequence 4 is marked by terrigenous sediments (shale). This is an incomplete aggradation sequence formed during the Burdigalian Age in the Andabad area (Figs. 6 and 12). The sequence mainly consisted of lagoon shale and was deposited at water depth ~13 m. The thickness of this sequence was 106 m. The sequence four is bounded from above by Type II sequence boundary. The bioclast Corallinaceae perforate-imperforate foraminifera wackestone-packstone (MF3) marks the boundary between this sequence and sequence 5. No evidence of erosion or incision could be observed at this sequence boundary in the Andabad area.

Sequence 5

Sequence 5 reaching 17 m in thickness was formed in the Andabad area during the Burdigalian Age (Figs. 6 and 12). The sequence consists primarily of limestone and commences with the bioclast corallinaceae perforate-imperforate foraminifera wackestone-packstone (MF3). Transgressive systems tract (TST) of this sequence included MFs 3, 4, and 5. The coral corallinaceae wackestone-packstone (MF5) marks the maximum flooding surface (MFS) of the sequence 5. The maximum water depth the during deposition this sequence has been estimated as ~19 m. Highstand systems tract (HST) was also identified with MFs1, 2, 3, 4, and 5. The sandy bioclast wackestone-packstone (MF1) marks the boundary between this sequence and sequence 6. Additionally, the lack of any evidence of erosion or incision suggests that it is a Type II sequence boundary.

Sequence 6

This sequence reaching 11-m-thick and consisting of limestone was formed in the Andabad area during the Burdigalian Age (Figs. 6 and 12). The bioclast Corallinaceae perforate-imperforate foraminifera wackestone-packstone (MF3) marks the beginning of this sequence. TST comprises

biofacies MF3. The sequence starts with limestones suggesting a lagoon environment. Maximum Flooding Surface (MFS) is lined by the bioclast pelagic foraminifera wackestone-packstone (MF9). In this sequence, the estimated maximum water depth exceeded ~25 m. The biofacies such as MFs 1, 3, and 5, were deposited as a highstand systems tract (HST). The boundary between this sequence and the sequence 7 is marked by the sandy bioclast wackestone-packstone (MF1). This sequence boundary (taking into account the absence of signs of erosion and incision) is a Type II sequence boundary.
Text-Fig. 12

Sequence 7

This sequence, 86 m in thickness, formed during the Burdigalian Age in the Andabad area (Figs. 6 and 13) consists primarily of limestones corresponding to inner and proximal middle shelf environments and commences with the bioclast corallinaceae perforate-imperforate foraminifera wackestone-packstone (MF3). This biofacies is succeeded by MFs 2, 3, 4, and 5 comprising the transgressive systems tract. The bioclast corallinaceae perforate foraminifera wackestone-packstone (MF6) marks the maximum flooding surface (MFS) when estimated water depth reached ~ 15m. Biofacies such as MFs 1, 2, 3, 4, 5, and 6 were deposited as a highstand systems tract (HST). The boundary between the Qom Formation and the Upper Red Formation is a Type I sequence boundary. No evidence of erosion has bee observed between the Qom Formation and the overlying Upper Red Formation in the Andabad area.
Text-Fig. 13

5.3 Correlation between Depositional Sequence of North/South Margin of Neotethys and Paratethys Basins

The Qom Basin was located on the northern margin of the Neotethys Basin (Harzhauser and Piller, 2007; Reuter et al., 2009). The Neotethys Basin itself was connected with the Paratethys Basin (Harzhauser and Piller, 2007). As a result, the present study attempted to correlate the depositional sequences formed in the Qom Basin with depositional sequences of the Asmari Formation (southern margin of Neotethys), as well as with depositional sequences formed in the

Paratethys Basin (Vakarcs et al., 1998; Ehrenberg et al., 2007; van Buchem et al., 2010) (Fig. 14). During the Aquitanian Age, two third-order depositional sequences and one aggradation sequence were formed in the Nowbaran area, and two depositional sequences were formed on the southern margin of Neotethys and Paratethys Basins. This indicates the activity of local faults during this Age. During the Burdigalian Age, three third-order depositional sequences and one incomplete (aggradation) depositional sequence were deposited in the Andabad area. The correlation between depositional sequences of the Andabad area and depositional sequences identified in the southern margin of Neotethys and Paratethys Basins show that, during the Burdigalian Age, the Qom Formation was more affected by sea level fluctuations on a global scale. In addition, presence of the third depositional sequence at the end of the Aquitanian Age in the Nowbaran area, as well as of the fourth depositional sequence at the beginning of the Burdigalian Age in the Andabad area suggests that lack of sea level fluctuations in the Qom Basin from the late Aquitanian Age to the early Burdigalian Age (Figs. 6 and 7).
Text-Fig. 14

6 Discussion

Several authors suggested that the deposition of the Qom Formation started at different times in the northern margin of the Neotethys Basin (Mohammadi et al., 2013). Therefore, the formation could be diachronous in different areas in the northern margin of the Neotethys Basin during the Oligocene–Miocene time (Mohammadi et al., 2013). This study deals with two sequences of the Qom Formation in different areas of the back-arc sub-basin (Qom basin), specifically in the Nowbaran area (Aquitanian age) and in the Andabad area (Burdigalian age). This formation in both studied areas was deposited in similar carbonate platform settings. However, the Qom Formation in the Nowbaran area was formed in a deeper environment compared to the Andabad area (Figs. 6 and 7). Additionally, Morley et al. (2009) suggested that local faults could be active in the northern margin of Neotethys Basin (Qom Basin) during the Oligocene and Miocene ages. In fact, the presence of the terrigenous facies (shales) of the Aquitanian age (the lower and upper sections of sequence in the Nowbaran area) and of the Burdigalian age (the lower section of sequence in the Andabad area) could be related to the activity of local faults and increasing terrigenous sediment input. The influence of local faults on the depositional sequences and the

position of sequence boundaries can be observed in the study areas (Fig. 14). In addition, the subsidence of the northern margin of the Neotethys Basin (Qom Basin) during the Oligocene and Miocene ages could be related to local fault activity (Morley et al., 2009). The activity of local faults is the reason for the observed inconsistencies in position of the sequence boundaries of to the depositional sequences in both studied areas, as well as in other studies (e.g. Vakarcs et al., 1998; Ehrenberg et al., 2007; van Buchem et al., 2010).

6 Conclusion

For the purpose of the present study, two sections in the Andabad and Nowbaran areas were selected. The Nowbaran area is located 3 km away from the southwest of Nowbaran city and northeast of Saveh city. The Anadabad area is located at 19 km away from northeast of Mahneshan city. With 122 (limestone) and 15 (shale) rock samples from the Andabad area and 94 (limestone) and 24 (shale) rock samples from the Nowbaran area, nine biofacies, one terrigenous facies, and five taphofacies have been identified in the studied areas. According to the vertical distribution of biofacies and the lack of bioclast, ooid, and reef barrier, an open-shelf carbonate platform can be considered for the Qom Formation in the studied areas. Open-shelf platform can be divided into three environments: inner shelf (restricted and semi-restricted lagoon), middle shelf, and outer shelf (open marine). Finally, seven depositional sequences have been identified, of which three belong to the Aquitanian Age and four belong to the Burdigalian Age.

Acknowledgments

The authors would like to thank the University of Isfahan for the financial support. This research did not receive any specific grant from funding agencies in the public, commercial, or not-for-profit sectors.

Reference

Abaie, I., Ansari, H.J., Badakhshan, A., Jaafari, A., 1964. History and development of the Alborz and Sarajeh fields of Central Iran. Bull. Iranian Petrol. Inst., 15, 561-574.

Abbassi, N., Domning, D.P., Izad, N.N., Shakeri, S., 2016. Sirenia fossils from Qom formation (Burdigalian) of the Kabudar Ahang Area, Northwest Iran. Riv. Ital. Paleontol. S., 122, 13–24.

Afzal, J., Williams, M., Leng, M.J., Aldridge, R.J., 2011. Dynamic response of the shallow marine benthic ecosystem to regional and pan-Tethyan environmental change at the Paleocene–Eocene boundary. Palaeogeogr. Palaeoclimatol. Palaeoecol., 309 (3): 141–160.

Aghanabati, A., 2006. Geology of Iran, Geological Survey of Iran, Teheran.

Allison, P.A., Bottjer, D.J., 2011. Taphonomy: process and bias through time, Springer, New York.

Amirshahkarami, M., Vaziri-Moghaddam, H., Taheri, A., 2007. Paleoenvironmental model and sequence stratigraphy of the Asmari Formation in southwest Iran. Historical. Biol., 19, 173–183.

Behforouzi, E., Safari, A., 2011. Biostratigraphy and paleoecology of the Qom Formation in the Chenar area (northwestern Kashan), Iran. Rev. Mex. Cienc. Geol., 28, 555–565.

Beavington-Penney, S.J., 2004. Analysis of the effects of abrasion on the test of Palaeonummulites venosus: implications for the origin of nummulithoclastic sediments. Palaios, 19, 143–155.

Beavington-Penney, S.J., Wright, V.P., Racey, A., 2006. The middle Eocene Seeb Formation of Oman: an investigation of acyclicity, stratigraphic completeness, and accumulation rates in shallow marine carbonate settings. J. Sediment. Res. A. Sediment. Petrol. Process, 76, 1137–1161.

Beavington-Penney, S.J., Wright, V.P., Woelkerling, W.J., 2004. Recognising macrophyte-vegetated environments in the rock record: a new criterion using ‘hooked’forms of crustose coralline red algae. Sediment. Geol., 166, 1–9.

Berberian, M., King, G.C.P., 1981. Towards a paleogeography and tectonic evolution of Iran. Can. J. Earth Sci., 18(2), 210–265.

Beresi, M.S., Cabaleri, N.G., Löser, H., Armella, C., 2016. Coral patch reef system and associated facies from southwestern Gondwana: paleoenvironmental evolution of the Oxfordian

shallow-marine carbonate platform at Portada Covunco, Neuquén Basin, Argentina. Facies, 63, 1–22.

Berning, B., Reuter, M., Piller, W.E., Harzhauser, M., Kroh, A., 2009. Larger foraminifera as a substratum for encrusting bryozoans (Late Oligocene, Tethyan Seaway, Iran). Facies, 55(2), 227–241

Bover-Arnal, T., Ferrandez-Canadell, C., Aguirre, J., Esteban, M., Fernandez-Carmona, J., Albert-Villanueva, E., Salas, R., 2017. Late Chattian platform carbonates with benthic foraminifera and coralline algae from the SE Iberian plate. Palaios, 32, 61–82.

Brachert, T.C., Betzler, C., Braga, J.C., Martin, J.M., 1998. Microtaphofacies of a warm-temperate carbonate ramp (uppermost Tortonian/lowermost Messinian, southern Spain). Palaios, 13, 459–475.

Brandano, M., Cornacchia, I., Raffi, I., Tomassetti, L., 2016. The Oligocene–Miocene stratigraphic evolution of the Majella carbonate platform (Central Apennines, Italy). Sediment. Geol., 333, 1–14.

Brandano, M., Lipparini, L., Campagnoni, V., Tomassetti, L., 2012. Downslope-migrating large dunes in the Chattian carbonate ramp of the Majella Mountains (Central Apennines, Italy). Sediment. Geol., 255, 29–41.

Catuneanu, O., Galloway, W., Kendall, C.H., Maill, H., Tucker, M., 2011. Sequence Stratigraphy: Methodology and Nomenclature. Newsl. Stratigr., 44,173–245.

Ćosović, V., Drobne, K., Ibrahimpašić, H., 2012. The role of taphonomic features in the palaeoecological interpretation of Eocene carbonates from the Adriatic carbonate platform (PgAdCP). Neues Jahrb. Geol. Paläontol., 265, 101–112.

Ehrenberg, S.N., Picard, N.A.H., Laursen, G.V., Monibi, S., Mossadegh, Z.K., Svana, T.A., , Aqrawi, A.A.M., McArthur, J.M., Thirlwall, M.F., 2007. Strontium isotope stratigraphy of the Asmari Formation (Oligocene – Lower Miocene), SW Iran. J. Petrol. Geol., 30, 107–128.

Daneshian, J., Dana, L.R., 2007. Early Miocene benthic foraminifera and biostratigraphy of the Qom Formation, Deh Namak, central Iran. J. Asian Earth Sci., 29, 844–858.

Daneshian, J., Ghanbari, M., 2017. Stratigraphic distribution of planktonic foraminifera from the Qom Formation: A case study from the Zanjan area (NW Central Iran). Neues Jahrb. Geol. P-A., 283, 239–254.

Dunham, R.J., 1962. Classification of carbonate rocks according to depositional texture, in: Ham, W.E., (Eds.), Classification of carbonate rocks: A symposium: American Association Petroleum Geologist, pp. 108–121.

Embry, A.F., Klovan, J.E., 1971. Late Devonian reef tract on northeastern Banks Island, Northwest territories. B. Can. Petrol. Geol., 19, 730–781.

Flugel, E., 1972. Mikrofazielle Untersuchungen in der alpinen Trias: Methoden und Probleme. Mitt. Ges. Geol. Bergbaustud., 21, 9–64.

Flugel, E., 1982. Microfacies analysis of limestones, Springer, Berlin.

Flugel, E., 2010. Microfacies of carbonate rocks, Springer, Berlin.

Furrer M.A., Soder P.A., 1955. The Oligo-Miocene marine formation in the Qum region (Central Iran) (with discussion). 4th World Petrol. Cong., Rome, sec., 1, 267–277.

Gansser, A., 1955. New aspects of the geology in Central Iran. Proceeding 4th World Petroleum Congress Rome section I/A/5, 279–300.

Geel, H., 2000. Recognition of stratigraphic carbonat platform and slope deposits: empirical models based on microfasies analysis of paleogene deposits in southestern Spain. Palaeogeogr. Palaeoclimatol. Palaeoecol., 1550, 211–238.

Greenstein, B.J., Pandolfi, J.M., 2003. Taphonomic alteration of reef corals: Effects of reef environment and coral growth form II: The Florida Keys. Palaios, 18, 495–509.

Hallock, P., 1999. Symbiont-bearing foraminifera. In Modern foraminifera. Springer, Dordrecht, 123–139.

Hallock, P., Glenn, E.C., 1986. Larger foraminifera: a tool for paleoenvironmental analysis of Cenozoic carbonate depositional facies. Palaios, 1, 55–64.

Hallock, P., Hansen, H.J., 1979. Depth adaptation in Amphistegina: change in lamellar thickness. Bull. Geol. Soc. Den., 27, 99–104.

Handford, C.R., Loucks, R.G., 1993. Carbonate depositional sequences and systems tracts-responses of carbonate platforms to relative sea level changes, in: Loucks, R.G., Sarg, J.F. (Eds.), Carbonate sequence stratigraphy – Recent developments and applications. AAPG Memoir, pp. 3–41

Haq, B.U., Shutter, S.R., 2008. Sequences (SEPM Global or Tethyan): TS Creator: Time Scale Creator [Internet]. 2005-2013. Geologic Time Scale Foundation. Available from: http//tscreator.com.

Harzhauser, M., 2004. Oligocene gastropod faunas of the eastern Mediterranean (mesohellenic trough/Greece and Esfahan-Sirjan Basin/central Iran). Cour. Forsch. Inst. Senckenberg, 248, 93–182.

Harzhauser, M., Piller, W.E., 2007. Benchmark data of a changing sea—palaeogeography, palaeobiogeography and events in the Central Paratethys during the Miocene. Palaeogeog. Palaeoclimatol. Palaeoecol., 253, 8–31

Heydari, E., 2008. Tectonics versus eustatic control on supersequences of the Zagros Mountains of Iran. Tectonophysics, 451(1–4), 56–70.

Jamshidi, K.H., Masoomi, R., Nozari, A., 2001. Geological map 1: 100,000 Mah Neshan the Geological survey and Mineral Exploration of Iran, Tehran.

Khaksar, K., Maghfouri Moghadam,, I., 2007. Paleontological study of the echinoderms in the Qom Formation (Central Iran). Earth Sci. Res. J., 11, 57–79.

Kiani, T., 2001. Geological map 1: 100,000 Mah Neshan the Geological survey and Mineral Exploration of Iran, Tehran.

Knoerich, A.C., Mutti, M., 2003. Controls of facies and sediment composition on the diagenetic pathway of shallow-water Heterozoan carbonates: the Oligocene of the Maltese Islands. Int. J. Earth. Sci., 92, 494–510.

Larsen, A.R., Drooger, C.W., 1977. Relative thickness of the test in the Amphistegina species of the Gulf of Elat. Utrecht. Micropaleontological. Bulletins, 15, 225–239.

Loftus, W.K., 1854. On the Geology of portions of the Turko-Persian Frontier, and of the Districts adjoining. Q. J. Geol. Soc., 10, 464–469.

Moghadam, M.Y., 2011. Early Oligocene larger foraminiferal biostratigraphy of the Qom Formation, south of Uromieh (NW Iran). Turkish J. Earth Sci., 20, 847–856.

Mohammadi, E., Safari, A., Vaziri-Moghaddam, H., Vaziri, M.R., Ghaedi, M., 2011. Microfacies analysis and paleoenviornmental interpretation of the Qom Formation, South of the Kashan, Central Iran. Carbonate. Evaporite., 26, 255–271.

Mohammadi, E., Hasanzadeh-Dastgerdi, M., Safari, A., Vaziri-Moghaddam, H., 2018. Microfacies and depositional environments of the Qom Formation in Barzok area, SW Kashan, Iran. Carbonate. Evaporite., 1, 1–14.

Mohammadi, E., Hasanzadeh-Dastgerdi, M., Ghaedi, M., Dehghan, R., Safari, A., Vaziri-Moghaddam, H., Baizidi, C., Vaziri, M.R., Sfidari, E., 2013. The Tethyan Seaway Iranian Plate

Oligo-Miocene deposits (the Qom Formation): distribution of Rupelian (Early Oligocene) and evaporate deposits as evidences for timing and trending of opening and closure of the Tethyan Seaway. Carbonate. Evaporite, 28, 321–345.

Morley, C.K., Kongwung, B., Julapour, A.A., Abdolghafourian, M., Hajian, M., Waples, D., Warren, J., Otterdoom, H., Srisuriyon, K., Kazemi, H., 2009. Structural development of a major late Cenozoic basin and transpressional belt in central Iran: The Central Basin in the Qom-Saveh area. Geosphere, 5, 325–362.

Mateu-Vicens, G., Hallock, P., Brandano, M., Demchuk, T., Gary, A., 2009, Test shape variability of Amphistegina d'Orbigny 1826 as a paleobathymetric proxy: application to two Miocene examples. Geologic problems solving with microfossils. J. Sediment. Res. A. Sediment. Petrol. Process., 93, 67–82.

Nebelsick, J.H., Bassi, D., 2000. Diversity, growth forms and taphonomy: key factors controlling the fabric of coralline algae dominated shelf carbonates. Geol. Soc. London Spec. Publ., 178, 89–107.

Nebelsick, J.H., Bassi, D., Lempp, J., 2013. Tracking paleoenvironmental changes in coralline algal-dominated carbonates of the Lower Oligocene Calcareniti di Castelgomberto formation (Monti Berici, Italy). Facies, 59, 133–148.

Nebelsick, J.H., Bassi, D., Rasser, M.W., 2011. Microtaphofacies: Exploring the Potential for Taphonomic Analysis in Carbonates, in: Allison, P.A., Bottjer, D.J. (Eds.), Taphonomy. Aims and Scope Topics in Geobiology Book Series, 32: Springer, Dordrecht, pp. 337–373.

Nadimi, A., 2007. Evolution of the Central Iranian basement. Gondwana. Res., 12, 324–333.

Pomar, L., 2001. Types of carbonate platforms: a genetic approach. Basin Research, 13, 313–334.

Pomar, L., Baceta, J.I., Hallock, P., Mateu-Vicens, G., Basso, D., 2017. Reef building and carbonate production modes in the west-central Tethys during the Cenozoic. Mar. Pet. Geol., 83, 261–304.

Pomar, L., Esteban, M., Martinez, W., Espino, D., De ott, V.C., Benkovics, L., Leyva, T.C., 2015. Oligocene–Miocene carbonates of the Perla Field, Offshore Venezuela: Depositional model and facies architecture, in: Bartolini, C., Mann, P. (Eds.), Petroleum geology and potential of the Colombian Caribbean margin. Am. Assoc. Pet. Geol., pp. 647–674.

Pomar, L., Mateu-Vicens, G., Morsilli, M., Brandano, M., 2014. Carbonate ramp evolution during the late Oligocene (Chattian), Salento Peninsula, southern Italy. Paleogeogr. Paleoclimatol. Paleoecol., 404, 109–132.

Rahiminejad, A.H., Nouradini, M., Yazdi, M., 2017. Palaeoenvironmental analysis of scleractinian reef corals from the Oligo–Miocene Qom Formation in the Vartun section (northeastern Esfahan, central Iran). Hist. Biol., 29, 384–394.

Read, J.F., 1982. Carbonate platforms of passive (extensional) continental margins: types, characteristics and evolution. Tectonophysics, 81, 195–212.

Read, J.F., 1985. Carbonate platform facies models. AAPG Bull., 69, 1–21.

Reuter, M., Piller, W.E., Harzhauser, M., Mandic, O., Berning, B., Rögl, F., Kroh, A., Aubry, M.P., Wielandt-Schuster, U., Hamedani, A., 2009. The Oligo-/Miocene Qom Formation (Iran): evidence for an early Burdigalian restriction of the Tethyan Seaway and closure of its Iranian gateways. Int. J. Earth. Sci., 98, 627–650.

Riegl, B., Poiriez, A., Janson, X., Bergman, K.L., 2010. The gulf: facies belts, physical, chemical, and biological parameters of sedimentation on a carbonate ramp. in: Westphal, H,, Reigl, B., Eberli, G.P., (Eds.), Carbonate Depositional Systems: Assessing Dimensions and Controlling Parameters. Springer, 1, pp. 145–213.

Renema, W., 2006. Large benthic foraminifera from the deep photic zone of a mixed siliciclastic-carbonate shelf off East Kalimantan, Indonesia. Mar. Micropaleontol., 58, 73–82.

Romero, J., Caus, E., Rosell, J., 2002. A model for the palaeoenvironmental distribution of larger foraminifera based on late Middle Eocene deposits on the margin of the South Pyrenean basin (NE Spain). Palaeogeogr. Palaeoclimatol. Palaeoecol., 179, 43–56.

Sarkar, S., 2017. Microfacies analysis of larger benthic foraminifera-dominated Middle Eocene carbonates: a palaeoenvironmental case study from Meghalaya, NE India (Eastern Tethys). Arab. J. Geosci., 5, 1–13.

Sarg, J.F., 1988. Carbonate sequence stratigraphy, in: Wilgus, C.K., Hastings, B.S., Kendall, C.G.St.C., Posamentier, H.W., Ross, C.A., Van Wagoner, J.C. (Eds.), Sea-Level Changes: An integrated approach: Soc Sediment. Geol. Spec. Pub., 43, 155–181.

Seddighi, M., Vaziri-Moghaddam, H., Taheri, A., Ghabeishavi, A., 2011. Depositional environment and constraining factors on the facies architecture of the Qom Formation, Central Basin, Iran. Hist. Biol., 24, 91–10.

Schuster, F., Wielandt, U., 1999. Oligocene and Early Miocene coral faunas from Iran: palaeoecology and palaeobiogeography. Int. J. Earth Sci., 88, 571–581.

Silvestri, G., Bosellini, F.R., Nebelsick, J.H., 2011. Microtaphofacies analysis of lower Oligocene turbid-water coral assemblages. Palaios, 26, 805–820.

Taheri, A., 2010. Paleoenvironmental model and sequence stratigraphy for the Oligo-Miocene foraminiferal limestone in east of Dogonbadan. Stratigr. Sedimentol., 40, 15–30.

Taheri, A., Vaziri-Moghaddam, H., Seyrafian, A., 2008. Relationships between foraminiferal assemblages and depositional sequences in Jahrum Formation, Ardal area (Zagros Basin, SW Iran). Hist. Biol., 20, 191–201.

Tomassetti, L., Benedetti, A., Brandano, M., 2016. Middle Eocene seagrass facies from Apennine carbonate platforms (Italy). Sediment. Geol., 335, 136–149.

van Buchem, F.S.P., Allan, T.L., Laursen, G.V., Lotfpour, M., Moallemi, A., Monibi, S., Motiei, H., Pickard, N.A.H., Tahmasbi, A.R., Vedrenne, V., Vincent, B., 2010. Regional stratigraphic architecture and reservoir types of the Oligo-Miocene deposits in the Dezful Embayment (Asmari and Pabdeh Formations), SW Iran. Geol. Soc. London Spec. Publ., 32, 219–263.

Vakarcs, G., Hardenbol, J., Abreu, V.S., Vail, P.R., Várnai, P., Tari, G., 1998. Oligocene-Middle Miocene depositional sequences of the central Paratethys and their correlation with regional stages. Geol. Soc. Am. Bull., 60, 209–231.

Van Wagoner, J.C., Posamentier, H.W., Mitchum, R.M.J.R., 1988. An overview of the fundamentals of sequence stratigraphy and key definition, in: Wilgus, C.K., Hastings, B.S., Kendall, C. G. St. C., Posamentier, H.W., Ross, C.A., Van Wagoner, J.C. (Eds.), Sea- Level Changes: An integrated approach: Geol. Soc. Am. Bull., 42, 39–45.

Vaziri-Moghaddam, H., Kimiagari, M., Taheri, A., 2006. Depositional environment and sequence stratigraphy of the Oligo-Miocene Asmari Formation in SW Iran. Facies, 52, 41–51.

Wilson, J.L., 1975. Carbonate facies in geologic history, Springer, New York.

Wilson, M.E., Evans, M.J., 2002. Sedimentology and diagenesis of Tertiary carbonates on the Mangkalihat Peninsula, Borneo: implications for subsurface reservoir quality. Mar. Pet. Geol., 19, 873–900.

Yazdi, M., Shirazi, M.P., Rahiminejad, A.H., Motavalipoor, R., 2012. Paleobathymetry and paleoecology of colonial corals from the Oligocene–early Miocene (?) Qom Formation (Dizlu area, central Iran). Carbonate. Evaporite., 27, 395–405.

Figure captions:

Fig. 1. Paleogeographic setting of the studied area. a, eight structural-sedimentary zones introduced by Heydari (2008); b, paleogeography map of the Tethyan seaway in Miocene (QB – Qom sub-basin; ESB – Esfahan-Sirjan sub-basin; UD – Urumieh-Dokhtar; ZB – Zagros Basin) (modified from Harzhauser and Piller, 2007; Reuter et al., 2009); c, schematic block diagram for the Esfahan-Sirjan and the Qom basins in the early Miocene time (modified from Reuter et al., 2009).

Fig. 2. Geological setting of the studied area. a, map of Iran; b, road map of the Nowbaran and Andabad areas; c, geological map of the Andabad area (after Kiani, 2001); d, geological map of the Nowbaran area (after Jamshidi et al., 2001).

Fig. 3. Biofacies types of the Qom Formation in the study areas. a, sandy bioclast wackestone-packstone MF-1; b, bioclast Corallinaceae imperforate foraminifera wackestone-packstone MF-2; c, bioclast Corallinaceae perforate-imperforate foraminifera wackestone-packstone MF-3; d, coral boundstone MF-4; e, coral Corallinaceae wackestone-packstone MF-5; f, bioclast Corallinaceae perforate foraminifera wackestone-packstone MF-6; g, bioclast corallinaceae pelagic-perforate foraminifera wackestone-packstone MF-7; h, bioclast pelagic benthic foraminifera wackestone-packstone MF-8; i, bioclast pelagic foraminifera wackestone-packstone MF-9. Abbreviations: B – bioclasts; Q – quartz grains; M – miliolids; Co – Corallinacean; S – *Sorites*; Am – *Amphistegina*; C – corals; Mi – *Miogypsina*; H – *Heterostegina*; P – planktonic foraminifera.

Fig. 4. Taphofacies of the Qom Formation in the Andabad area. a, MTF 1; b, MTF 2; c, MTF 3; d, MTF 4; e, MTF 5. Abbreviations: F – fragmentation; E – encrustation; A – abrasion.

Fig. 5. Taphofacies of the Qom Formation in the Nowbaran area. a, MTF 2; b, MTF 3; c, MTF 4; d, MTF 5. Abbreviations: F – fragmentation; E – encrustation; A – abrasion.

Fig. 6. Vertical biofacies distribution and sequences of the Qom Formation at the Andabad area (Northeast of Mah Neshan), Iran.

Fig. 7. Vertical biofacies distribution and sequences of the Qom Formation at the Nowbaran area (Northeast of Saveh), Iran.

Fig. 8. Depositional model for the platform carbonates of the Qom Formation in the Andabad and Nowbaran areas.

Fig. 9. Outcrop view of the first depositional sequence in the Nowbaran area.

Fig. 10. Outcrop view of the second depositional sequence in the Nowbaran area.

Fig. 11. Outcrop view of the third depositional sequence in the Nowbaran area.

Fig. 12. General view of the first, second, and third depositional sequence in the Andabad area.

Fig. 13. Outcrop view of the fourth depositional sequence in the Andabad area.

Fig. 14. Correlation of depositional sequences between south Tethyan seaway basin and the Paratethys basin with the studied areas.

Table captions:

Sample	Thickness (T), mm	Diameter (D), mm	Thickness/Diameter (T/D)	Depth, m	Biofacies
3e	0/55	1/2	0/45	~13	MF 3
35m	0/5	1/23	0/4	~19	MF 5
4v	0/44	1/2	0/36	~25	MF 6

Table 1. *Amphistegina* T/D measurements in the Andabad area.

Sample	Thickness (T), mm	Diameter (D), mm	Thickness/Diameter (T/D)	Depth, m	Biofacies
22	0/031	0/1	0/31	~34/5	MF 8
62	0/4	1/2	0.33	~30	MF 7
52	0/7	2/1	0/33	~30	MF 6
53	0/6	1/75	0/34	~29	MF 5
32	0/8	2	0/4	~19	MF 4
86	0/55	0/85	0/64	~8/5	MF 3

Table 2. *Amphistegina* T/D measurements in the Nowbaran area.

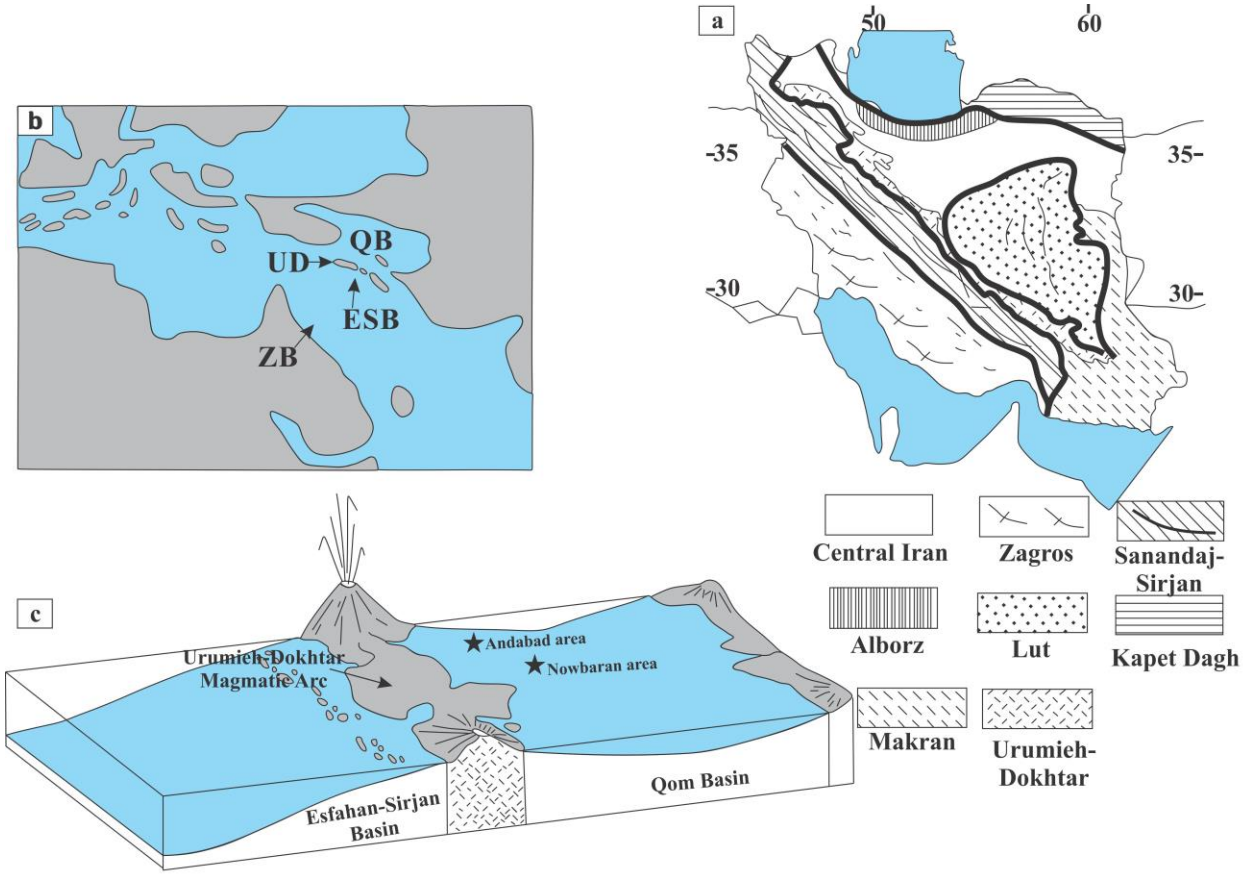
a
50
60
35
30
Central Iran
Zagros
Sanandaj-Sirjan
Alborz
Lut
Kapet Dagh
Makran
Urumieh-Dokhtar
b
QB
UD
ESB
ZB
c
Urumieh-Dokhtar Magmatic Arc
Andabad area
Nowbaran area
Esfahan-Sirjan Basin
Qom Basin

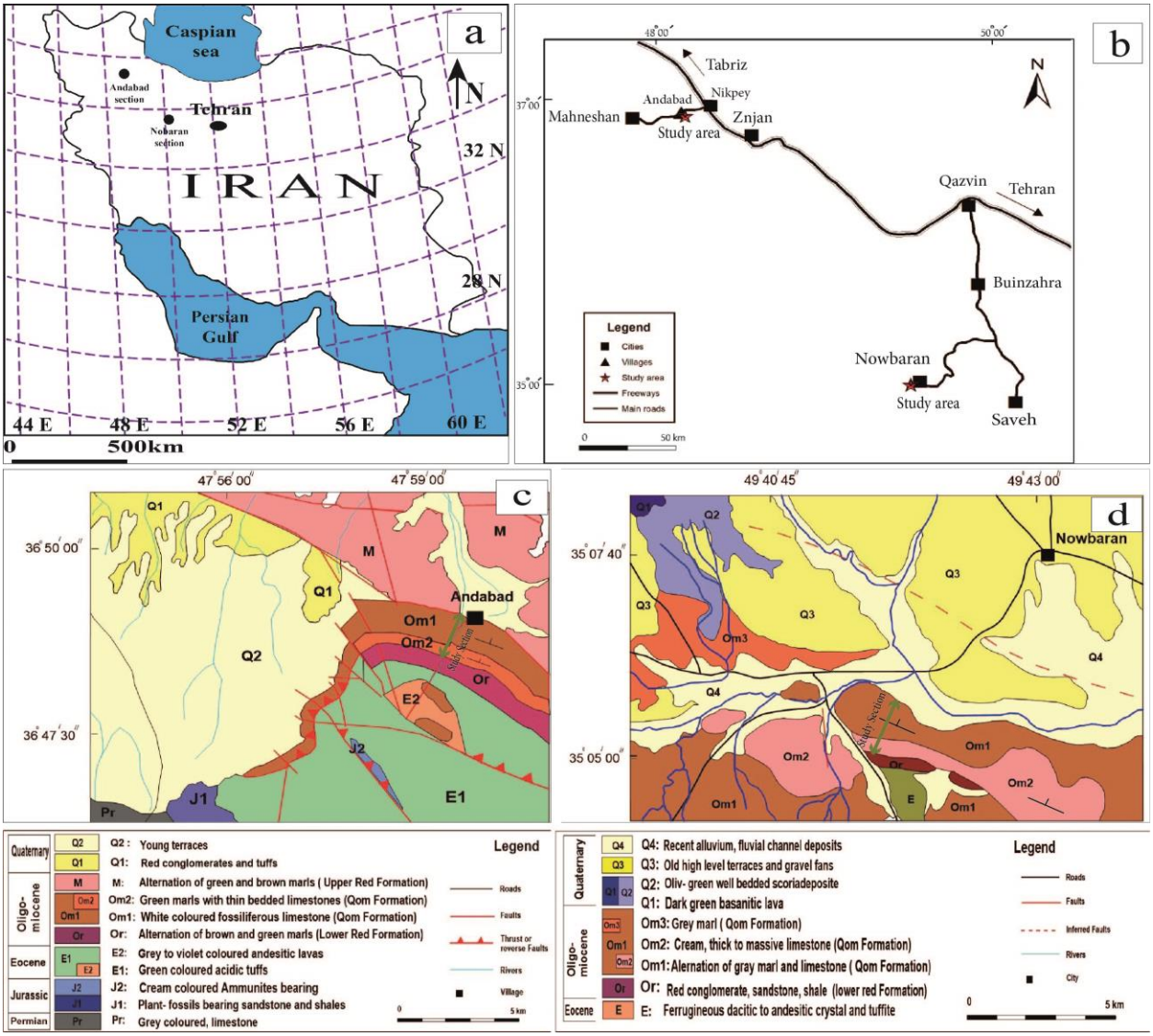
a
Caspian sea
Andabad section
Tehran
Nobaran section
IRAN
Persian Gulf
N
32 N
28 N
44 E
48 E
52 E
56 E
60 E
0
500km
b
48° 00′
50° 00′
37° 00′
Tabriz
Nikpey
Andabad
Mahneshan
Study area
Znjan
Qazvin
Tehran
Buinzahra
Nowbaran
Study area
Saveh
Legend
Cities
Villages
Study area
Freeways
Main roads
0
50 km
c
47° 56′ 00″
47° 59′ 00″
36° 50′ 00″
36° 47′ 30″
Q1
M
Andabad
Om1
Om2
Or
E2
J2
J1
E1
Pr
Q2
Strati Section
d
49° 40′ 45″
49° 43′ 00″
35° 07′ 40″
35° 05′ 00″
Nowbaran
Q2
Q3
Om3
Q4
Om2
Om1
Or
E
Strati Section
Quaternary
Oligo-miocene
Eocene
Jurassic
Permian
Q2 : Young terraces
Q1: Red conglomerates and tuffs
M: Alternation of green and brown marls (Upper Red Formation)
Om2: Green marls with thin bedded limestones (Qom Formation)
Om1: White coloured fossiliferous limestone (Qom Formation)
Or: Alternation of brown and green marls (Lower Red Formation)
E2: Grey to violet coloured andesitic lavas
E1: Green coloured acidic tuffs
J2: Cream coloured Ammunites bearing
J1: Plant- fossils bearing sandstone and shales
Pr: Grey coloured, limestone
Legend
Roads
Faults
Thrust or reverse Faults
Rivers
Village
0
5 km
Q4: Recent alluvium, fluvial channel deposits
Q3: Old high level terraces and gravel fans
Q2: Oliv- green well bedded scoriadeposite
Q1: Dark green basanitic lava
Om3: Grey marl (Qom Formation)
Om2: Cream, thick to massive limestone (Qom Formation)
Om1: Alernation of gray marl and limestone (Qom Formation)
Or: Red conglomerate, sandstone, shale (lower red Formation)
E: Ferrugineous dacitic to andesitic crystal and tuffite
Legend
Roads
Faults
Inferred Faults
Rivers
City
0
5 km

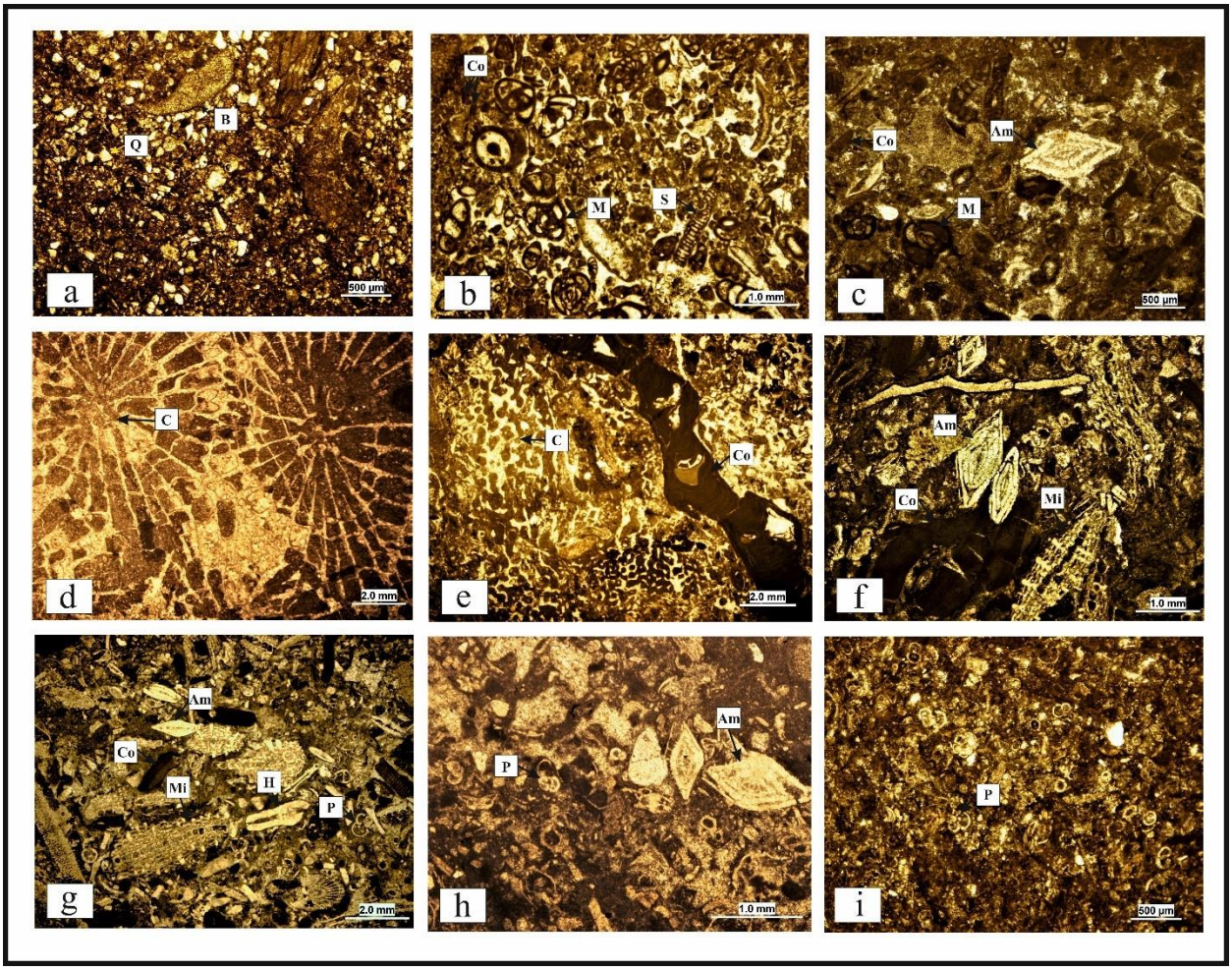
a
Q
B
500 µm
b
Co
M
S
1.0 mm
c
Co
Am
M
500 µm
d
C
2.0 mm
e
C
Co
2.0 mm
f
Am
Co
Mi
1.0 mm
g
Am
Co
Mi
II
P
2.0 mm
h
Am
P
1.0 mm
i
P
500 µm

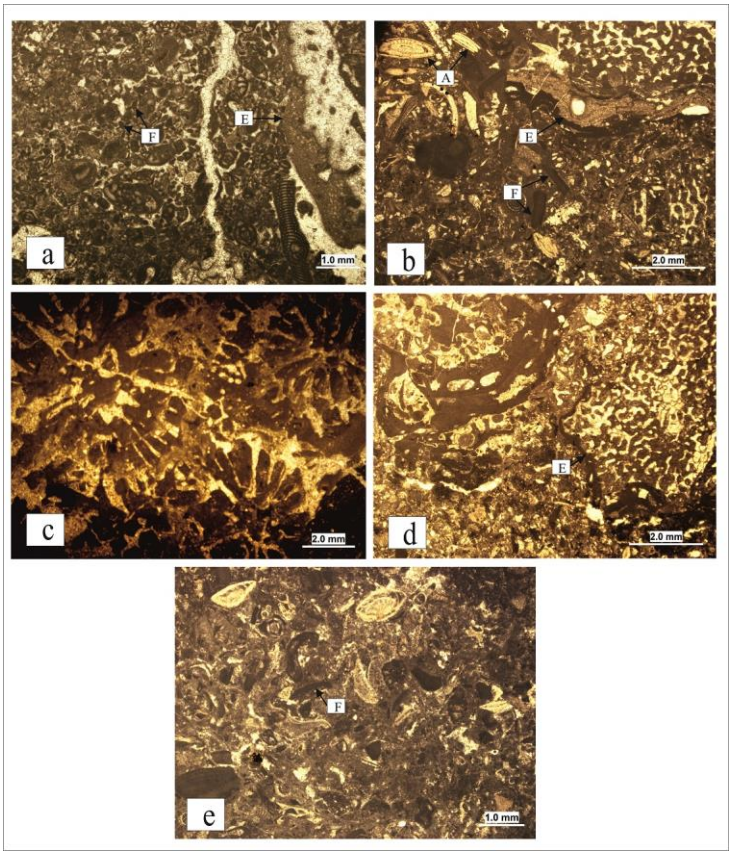
a
F
E
1.0 mm
b
A
E
F
2.0 mm
c
2.0 mm
d
E
2.0 mm
e
F
1.0 mm

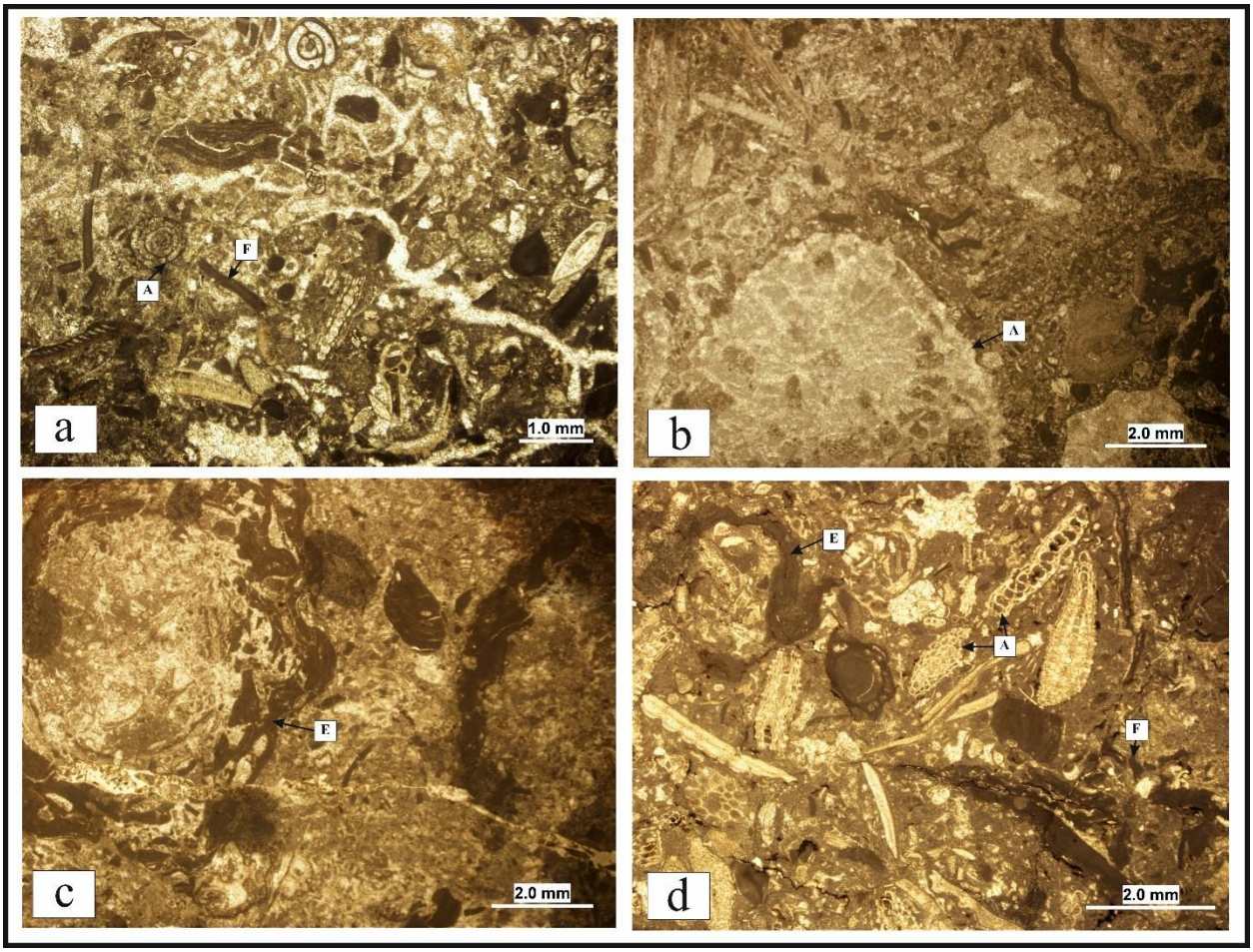
a
A
F
1.0 mm
b
A
2.0 mm
c
E
2.0 mm
d
E
A
F
2.0 mm

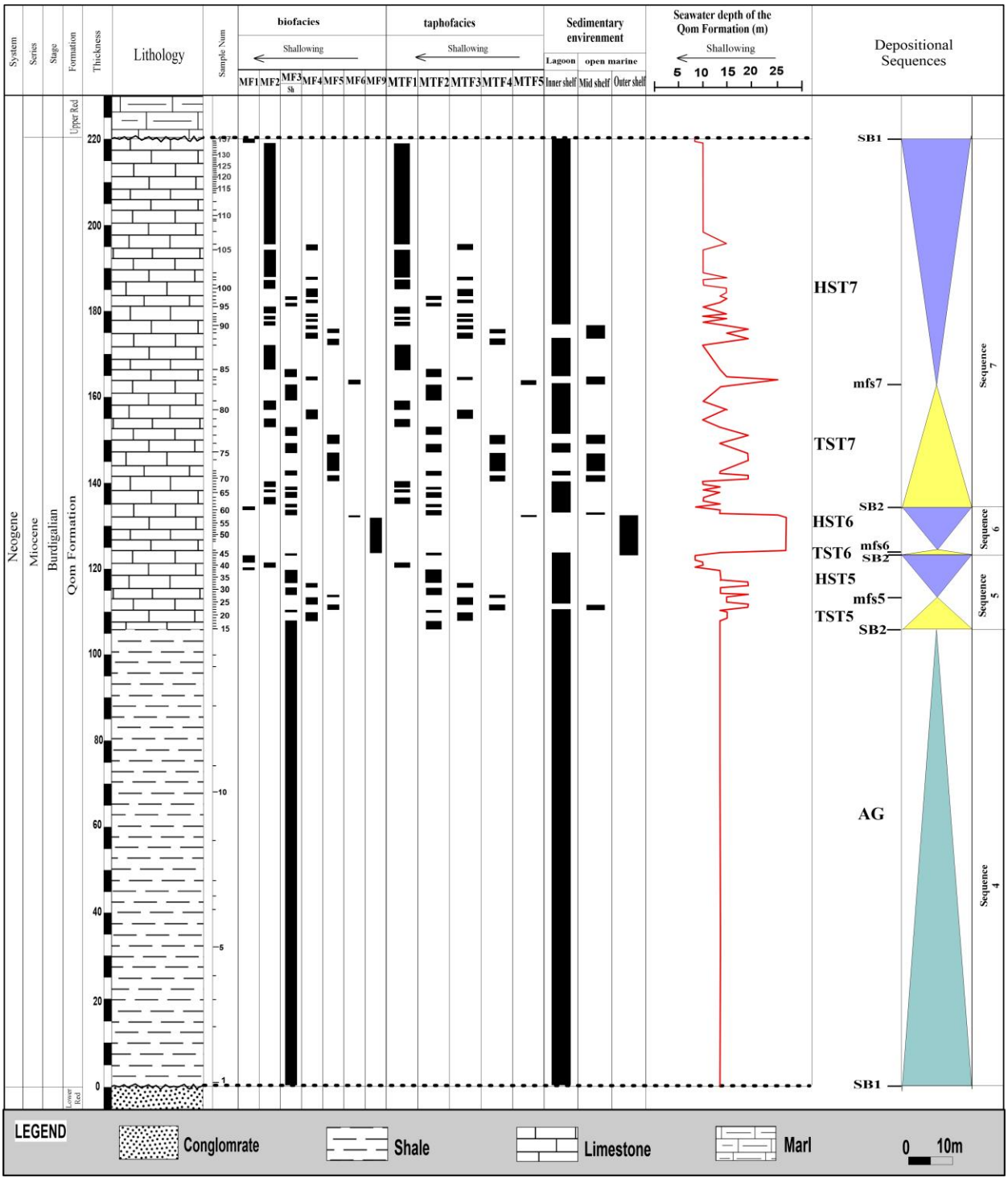
System
Series
Stage
Formation
Thickness
Lithology
Sample Num
biofacies
Shallowing
MF1 MF2 MF3 Sh MF4 MF5 MF6 MF9
taphofacies
Shallowing
MTF1 MTF2 MTF3 MTF4 MTF5
Sedimentary envirenment
Lagoon
open marine
Inner shelf
Mid shelf
Outer shelf
Seawater depth of the Qom Formation (m)
Shallowing
5 10 15 20 25
Depositional Sequences
Neogene
Miocene
Burdigalian
Qom Formation
Upper Red
Lower Red
SB1
HST7
mfs7
TST7
SB2
HST6
TST6
mfs6
SB2
HST5
mfs5
TST5
SB2
AG
SB1
Sequence 7
Sequence 6
Sequence 5
Sequence 4
LEGEND
Conglomrate
Shale
Limestone
Marl
0 10m

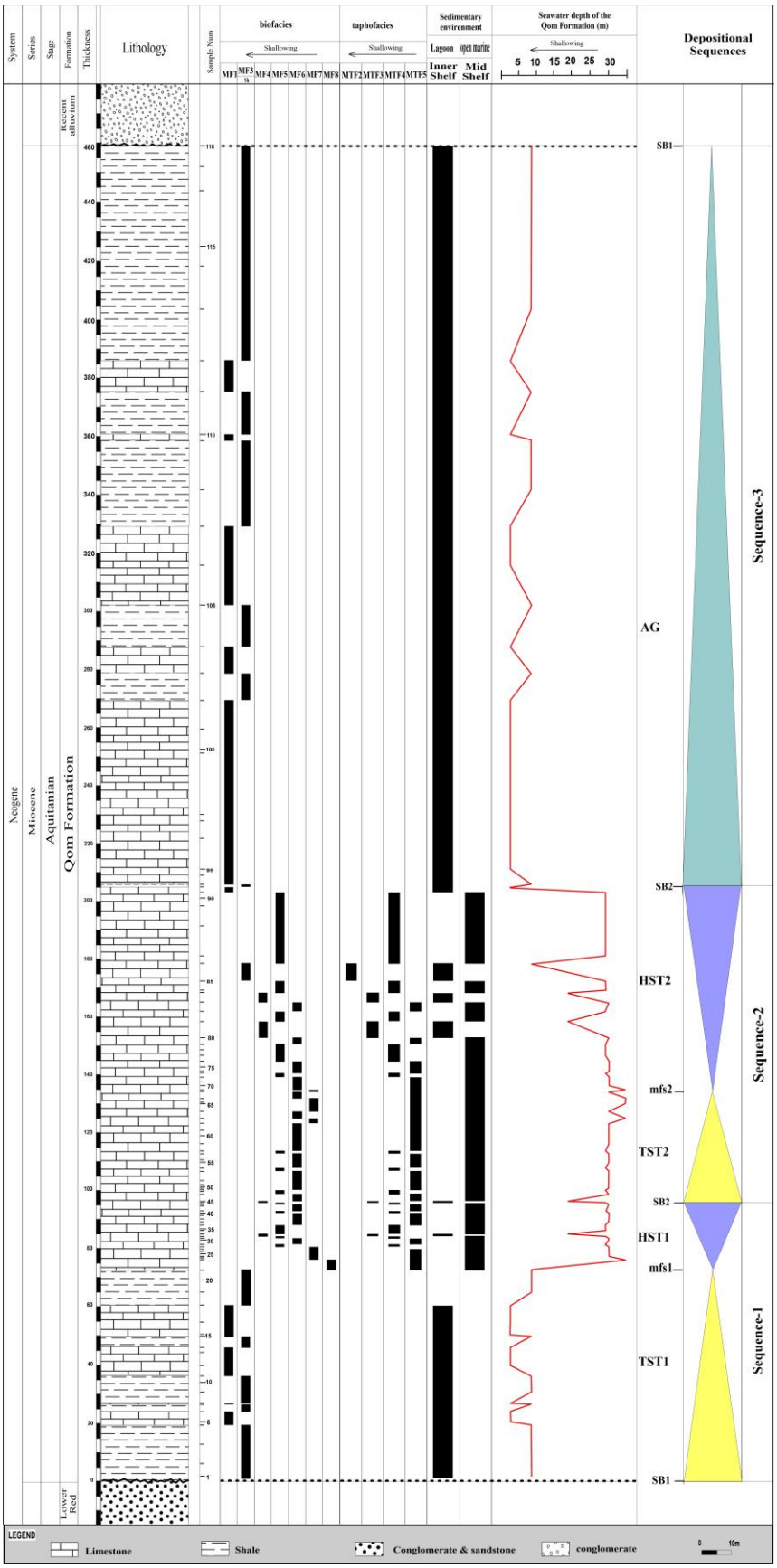
System
Series
Stage
Formation
Thickness
Lithology
Sample Num
biofacies
taphofacies
Sedimentary environment
Seawater depth of the Qom Formation (m)
Depositional Sequences
Shallowing
MF1
MF3
MF4
MF5
MF6
MF7
MF8
MTF2
MTF3
MTF4
MTF5
Lagoon
open marine
Inner Shelf
Mid Shelf
5 10 15 20 25 30
Neogene
Miocene
Aquitanian
Qom Formation
Recent alluvium
Lower Red
SB1
AG
SB2
HST2
mfs2
TST2
SB2
HST1
mfs1
TST1
SB1
Sequence-3
Sequence-2
Sequence-1
LEGEND
Limestone
Shale
Conglomerate & sandstone
conglomerate
0 10m

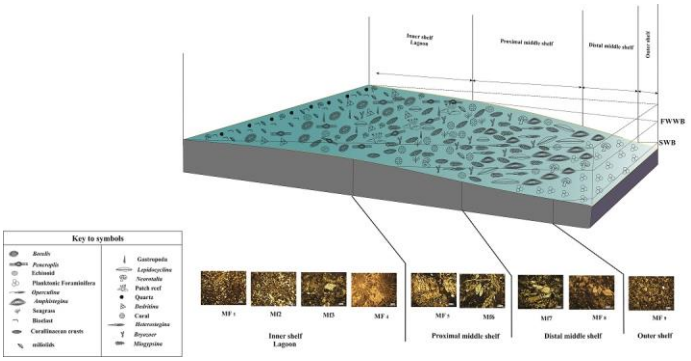
Inner shelf
Lagoon
Proximal middle shelf
Distal middle shelf
Outer shelf
FWWB
SWB
Key to symbols
Benthi
Foraminifera
Echinoid
Planktonic Foraminifera
Operculina
Amphistegina
Seagrass
Bioclast
Coralline
Gastropoda
Lepidocyclina
Nummulite
Patch reef
Quartz
Bedrock
Coral
Heterostegina
Bryozoan
Miogypsina
MF 1
MF2
MF3
MF 4
MF 5
MF6
MF7
MF 8
MF 9
Inner shelf
Lagoon
Proximal middle shelf
Distal middle shelf
Outer shelf

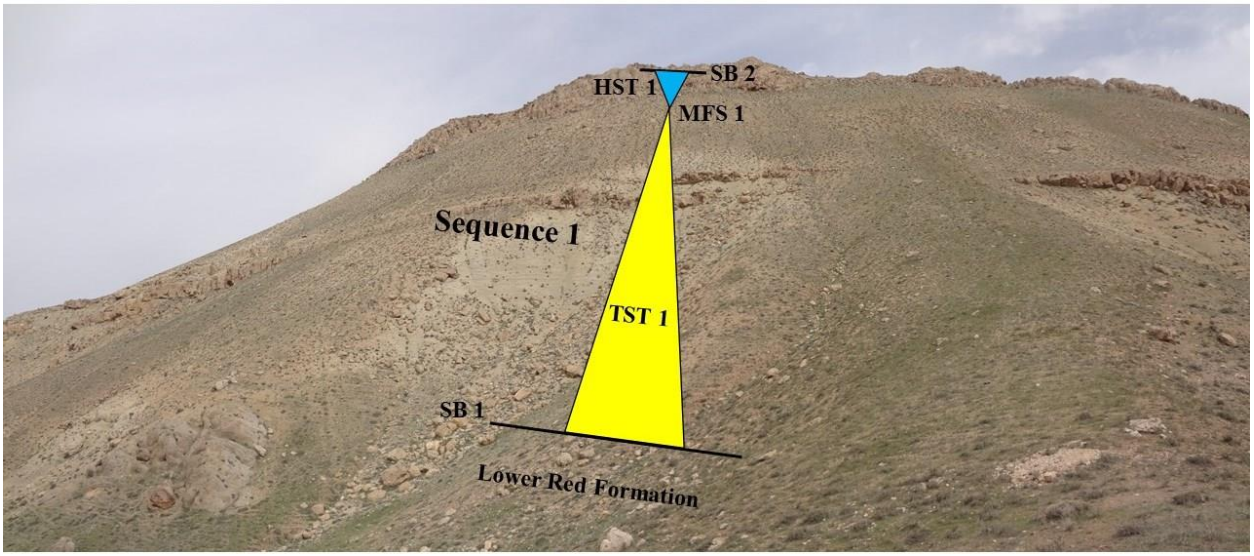
HST 1
SB 2
MFS 1
Sequence 1
TST 1
SB 1
Lower Red Formation

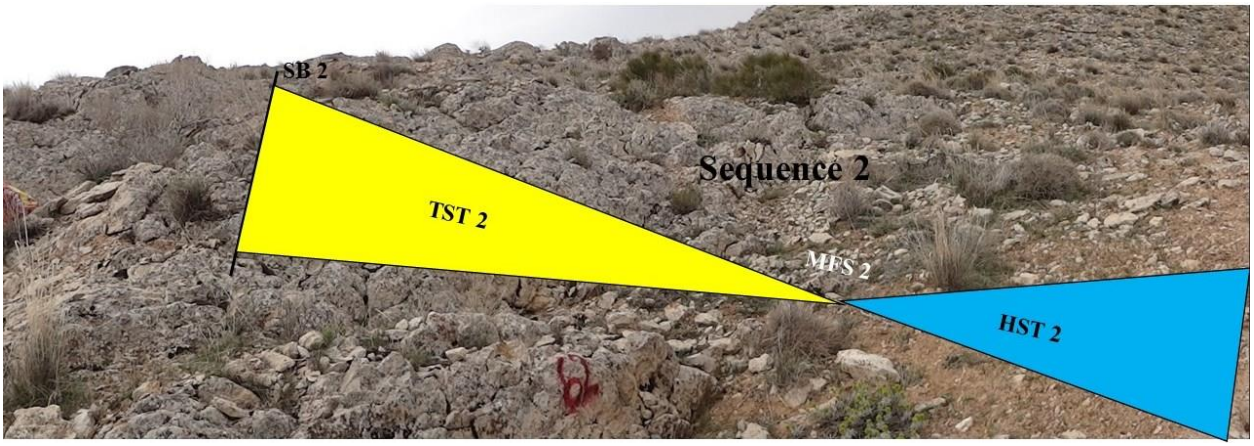
SB 2
Sequence 2
TST 2
MFS 2
HST 2

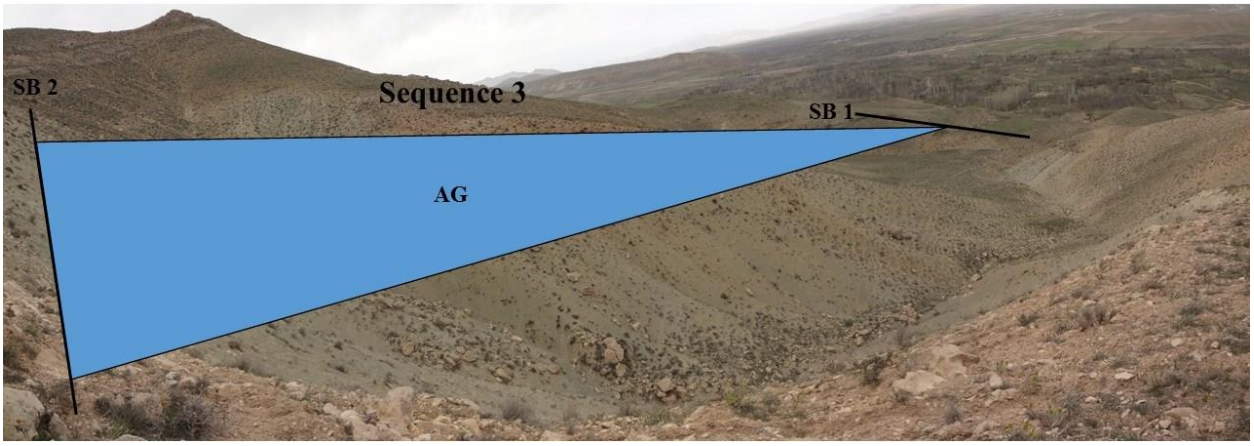
SB 2
Sequence 3
SB 1
AG

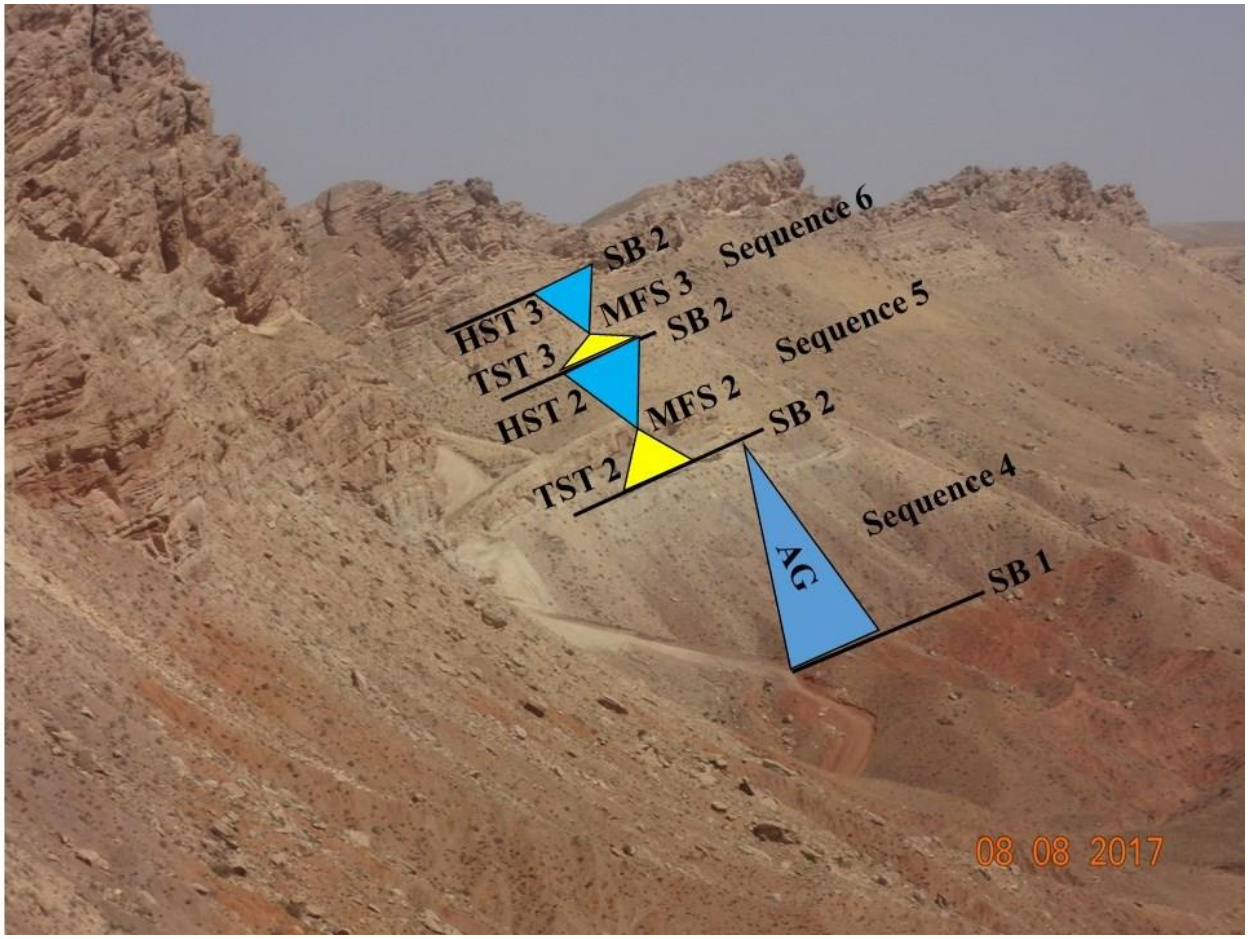
SB 2
Sequence 6
HST 3
MFS 3
SB 2
TST 3
Sequence 5
HST 2
MFS 2
SB 2
TST 2
Sequence 4
AG
SB 1
08 08 2017

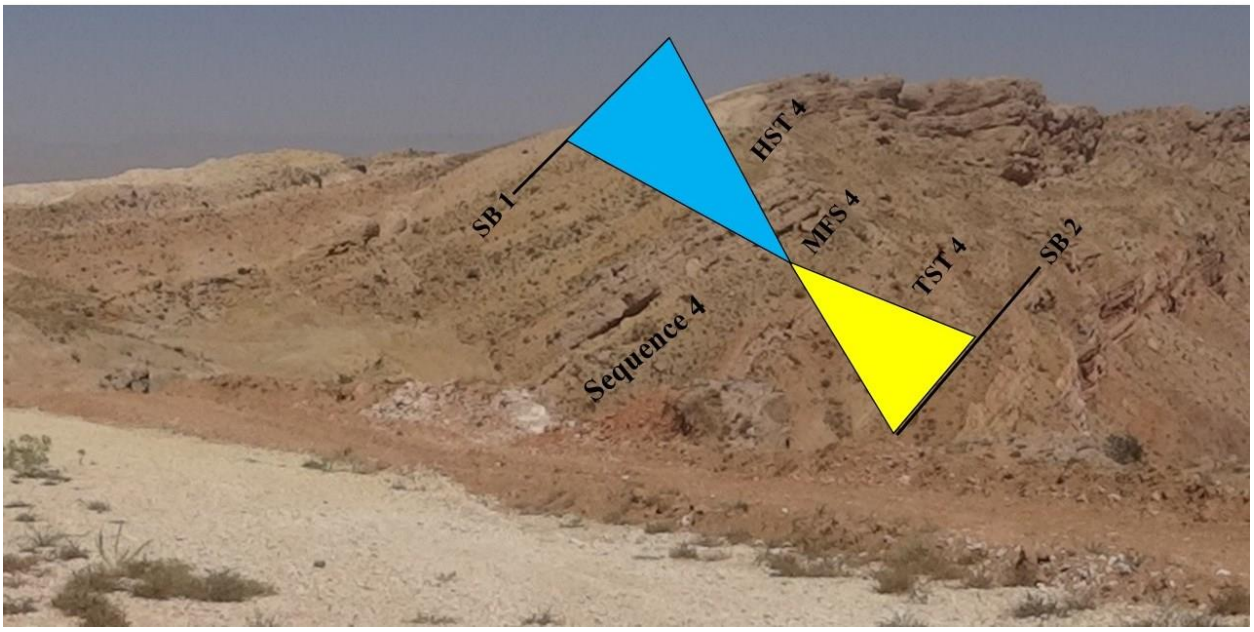
HST 4
SB 1
MFS 4
TST 4
SB 2
Sequence 4

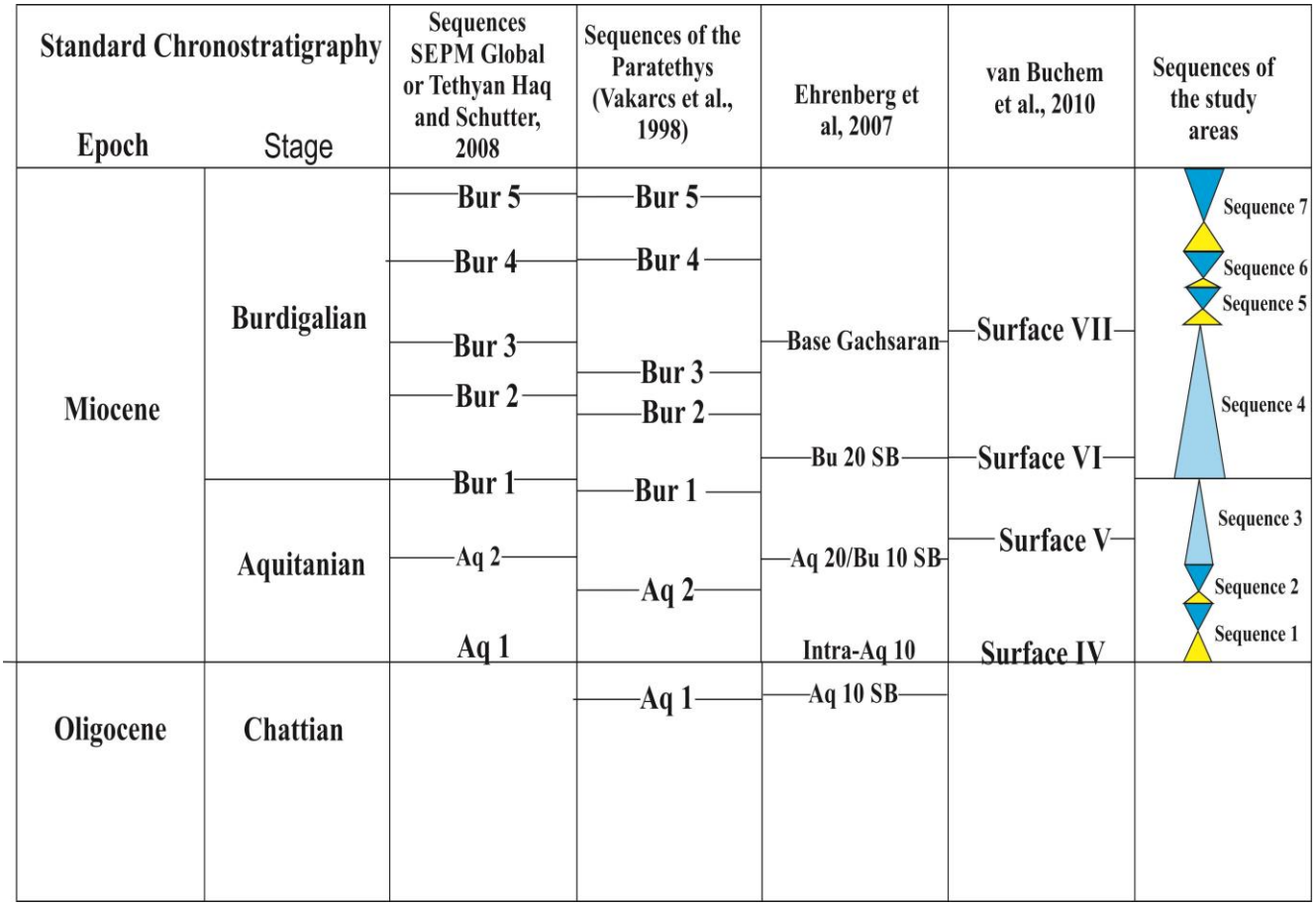
Standard Chronostratigraphy
Epoch
Stage
Sequences SEPM Global or Tethyan Haq and Schutter, 2008
Sequences of the Paratethys (Vakarcs et al., 1998)
Ehrenberg et al, 2007
van Buchem et al., 2010
Sequences of the study areas
Miocene
Burdigalian
Aquitanian
Oligocene
Chattian
Bur 5
Bur 4
Bur 3
Bur 2
Bur 1
Aq 2
Aq 1
Base Gachsaran
Bu 20 SB
Aq 20/Bu 10 SB
Intra-Aq 10
Aq 10 SB
Surface VII
Surface VI
Surface V
Surface IV
Sequence 7
Sequence 6
Sequence 5
Sequence 4
Sequence 3
Sequence 2
Sequence 1